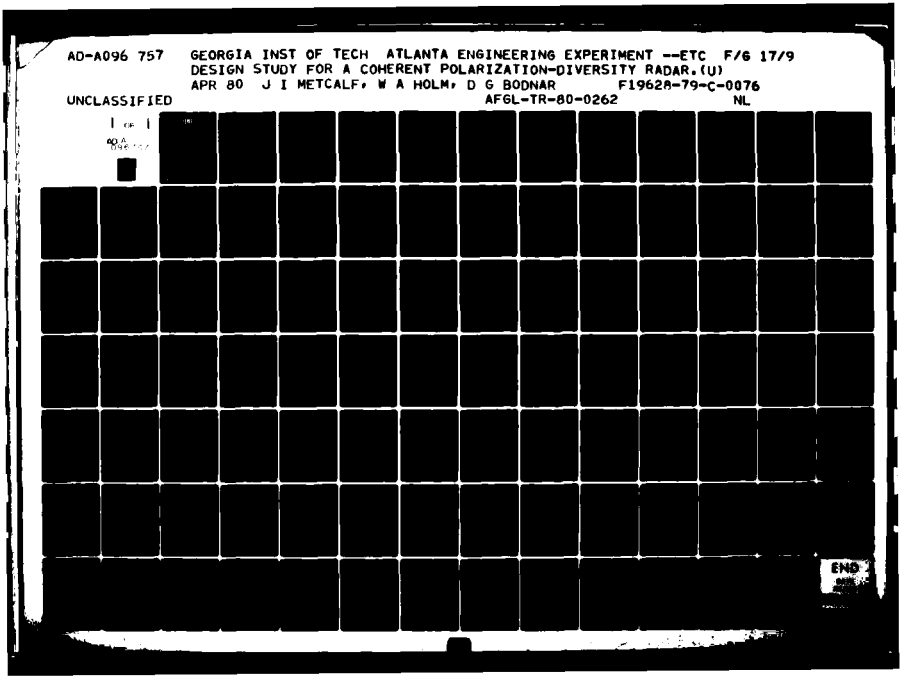
AD-A096 757 GEORGIA INST OF TECH ATLANTA ENGINEERING EXPERIMENT --ETC F/G 17/9
DESIGN STUDY FOR A COHERENT POLARIZATION-DIVERSITY RADAR,(U)
APR 80 J I METCALF, W A HOLM, D G BODNAR F19628-79-C-0076
UNCLASSIFIED AFGL-TR-80-0262 NL
END

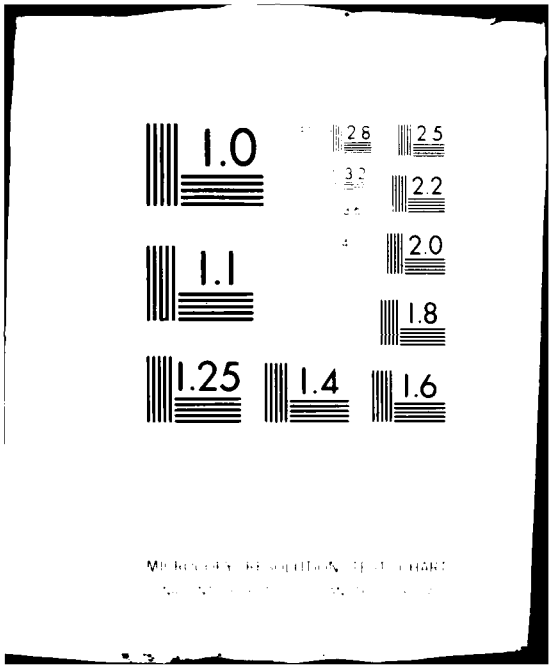
1.0
2.8
2.5
3.2
2.2
2.0
1.1
1.8
1.25
1.4
1.6

AFGL-TR-80-0262

DESIGN STUDY FOR A COHERENT POLARIZATION-DIVERSITY RADAR

James I. Metcalf
William A. Holm
Donald G. Bodnar
Edward E. Martin
Robert N. Trebits
William J. Steinway

GEORGIA INSTITUTE OF TECHNOLOGY
Engineering Experiment Station
Atlanta, Georgia 30332

April 30, 1980

Final Report for the Period
1 March 1979 - 11 April 1980

Approved for public release; distribution unlimited

Prepared for

AIR FORCE GEOPHYSICS LABORATORY
Air Force Systems Command
United States Air Force
Hanscom AFB, Massachusetts 01731

UNCLASSIFIED

SECURITY CLASSIFICATION OF THIS PAGE (When Data Entered)

(19) REPORT DOCUMENTATION PAGE		READ INSTRUCTIONS BEFORE COMPLETING FORM
(18) 1. REPORT NUMBER AFGL-TR-80-0262	2. GOVT ACCESSION NO. AD-A096 757	3. RECIPIENT'S CATALOG NUMBER
(6) (1) 4. TITLE (and Subtitle) Design Study for a Coherent Polarization-Diversity Radar •		(9) 5. TYPE OF REPORT & PERIOD COVERED Final rept. 1 Mar 1979-11 Apr 1980, 6. PERFORMING ORG. REPORT NUMBER
(10) 7. AUTHOR(s) James I. Metcalf, William A. Holm, Donald G. Bodnar, Edward E. Martin, Robert N. Trebits, and William J. Steinway		(15) 8. CONTRACT OR GRANT NUMBER(s) F19628-79-C-0076
9. PERFORMING ORGANIZATION NAME AND ADDRESS Engineering Experiment Station Georgia Institute of Technology Atlanta GA 30332		(16) 10. PROGRAM ELEMENT, PROJECT, TASK AREA & WORK UNIT NUMBERS 62101F 667007AB (17) 07
11. CONTROLLING OFFICE NAME AND ADDRESS Air Force Geophysics Laboratory (LYW) Hanscom AFB MA 01731 Monitor: K. M. Glover/LYW	(11)	12. REPORT DATE 30 Apr 1980 13. NUMBER OF PAGES 88
14. MONITORING AGENCY NAME & ADDRESS (If different from Controlling Office) (12) 95		15. SECURITY CLASS. (of this report) Unclassified 15a. DECLASSIFICATION/DOWNGRADING SCHEDULE

16. DISTRIBUTION STATEMENT (of this Report)

Approved for public release; distribution unlimited

17. DISTRIBUTION STATEMENT (of the abstract entered in Block 20, if different from Report)

18. SUPPLEMENTARY NOTES

19. KEY WORDS (Continue on reverse side if necessary and identify by block number)

Radar meteorology
Polarization-diversity radar
Cloud measurement
Precipitation measurement
Radar backscatter

20. ABSTRACT (Continue on reverse side if necessary and identify by block number)

Design concepts for a coherent polarization-diversity radar are presented. The desired capability is the measurement of microphysical parameters of hydrometeors, including thermodynamic phase, shape, size, orientation, and number density. The postulated use of a polarization-diversity radar is based on the relationships of these parameters to the anisotropy of the scattering and propagation media. The measurement objectives lead to the specification of primary and secondary coverage regions. Target detection within the primary region (less than 40 km range) and propagation effects lead to the →

DD FORM 1 JAN 73 1473 EDITION OF 1 NOV 65 IS OBSOLETE

UNCLASSIFIED

SECURITY CLASSIFICATION OF THIS PAGE (When Data Entered)

153850

BLOCK 20 (continued)

specification of S-band and K_a-band as optimum frequency bands for observations of precipitation and clouds, respectively. Radar system parameters are specified, and schematic diagrams of system hardware are presented. Antenna design concepts and practical considerations are discussed. We discuss concepts of data processing and a possible computer-oriented implementation of radar control and data processing.

TABLE OF CONTENTS

LIST OF ILLUSTRATIONS

LIST OF ILLUSTRATIONS (continued)

LIST OF TABLES

SECTION I
INTRODUCTION

Meteorological operations and research, as well as the operation of a variety of military weapons and communication systems, require detailed knowledge of the state of the atmosphere. Of concern for many applications are the bulk parameters of clouds and precipitation, such as rainfall (or snowfall) rate, total water content, and propagation parameters. Increasing sophistication of military systems and meteorological models requires increasing information to characterize cloud and precipitation media. Thus, there is a need for information concerning the thermodynamic phase, shape, size, orientation, and number density of hydrometeors. Past research has shown that these parameters are amenable to measurement, in varying degrees of accuracy, by polarization radar techniques. The concept underlying this approach is that the hydrometeor microphysical parameters are related to the anisotropy of either the scattering medium or the propagation medium and hence can be deduced from measurements by a dual-channel or dual-polarization radar. A theory for the use of non-coherent dual-channel radars for meteorological measurements was developed by McCormick and Hendry[1] and extended to coherent radars by Metcalf and Echard[2].

In addition to this major theoretical work, several experimental programs have been undertaken to measure various microphysical and bulk parameters. These have aimed at identification of hail in severe storms, improved accuracy of rainfall measurement through a parameterized drop size distribution, and the

[1] McCormick, G. C., and Hendry, A., 1975: Principles for the Radar Determination of the Polarization Properties of Precipitation. Radio Sci., 10, 421-434.

[2] Metcalf, J. I., and Echard, J. D., 1978: Coherent Polarization-Diversity Radar Techniques in Meteorology. J. Atmos. Sci., 35, 2010-2019.

documentation of signal propagation phenomena. Results of many theoretical and experimental programs were reviewed by Metcalf, et al.[3]

On the basis of past research we have developed radar system designs for the remote measurement of the microphysical parameters listed above. Key design factors include the operating frequency, pulse characteristics, power, and scanning capability. These are determined largely by the characteristics of the targets and the intended operational procedures. The constraints of scanning geometry, target properties, and radar parameters determine the output characteristics and the requirements for data processing and display. An important feature of the system is that it be coherent, to permit measurements of wind and turbulence (as is accomplished by single-channel coherent radars), and to determine the dependence of the scatterer anisotropy on Doppler frequency, through the two power spectra and the cross-spectrum of the two signals from the dual-channel receiver.

In presenting the system designs we begin with an overview of target characteristics and scanning geometries, then discuss measurement ambiguities and limits of spatial resolution and quantitative accuracy. We present the parameters for two radar systems, each of which is capable of achieving some of the measurement objectives. We discuss output data characteristics in general terms and present schematic diagrams of system hardware.

The theory of polarization-diversity radar discussed elsewhere will not be developed in detail in this report. Nomenclature and symbols used herein are consistent with those used previously and by other authors and are defined only to the extent required for this presentation.

[3] Metcalf, J. I., Brookshire, S. P., and Morton, T. P., 1978: Polarization-Diversity Radar and Lidar Technology in Meteorological Research: A Review of Theory and Measurements, AFGL-TR-78-0030, Air Force Geophysics Laboratory.

SECTION II
TARGET CHARACTERISTICS

The microphysical parameters listed in Section I are discussed below in the context of five meteorological target classifications: rain, snow, hail, cloud water, and cloud ice. Because of the various scattering, depolarization, and fall speed characteristics of these targets, they are amenable in varying degrees to measurement of the parameters of interest. While we do not intend to present a comprehensive review in this section of calculations and measurements reviewed elsewhere,[3] it is useful to relate radar-measurable parameters to the microphysical parameters before proceeding to discuss other aspects of the system designs.

A. RAIN

Rain is unique among the target classifications in having well-defined relationships of scattering cross section, shape, and fall speed to drop size. Because of these relationships the reflectivity-weighted average shape and, hence, size can be obtained from either the ratio of circularly polarized backscattered signals (from circularly polarized transmission) or the ratio of reflectivities measured at two linear polarizations aligned with the maximum and minimum dimensions of the drops. Figure 1 shows the relationships of circular depolarization ratio (CDR - the inverse of the cancellation ratio) to rainfall rate (for an assumed drop size distribution) and to drop size (D), based on computations by Humphries[4], McCormick and Hendry[1], and Warner and Rogers[5].

[4] Humphries, R. G., 1974: Depolarization Effects at 3 GHz due to Rain. Scientific Report MW-82, Stormy Weather Group, McGill University.

[5] Warner, C. W., and Rogers, R. R., 1977: Polarization-Diversity Radar: Two Theoretical Studies. Scientific Report MW-90, Stormy Weather Group, McGill University.

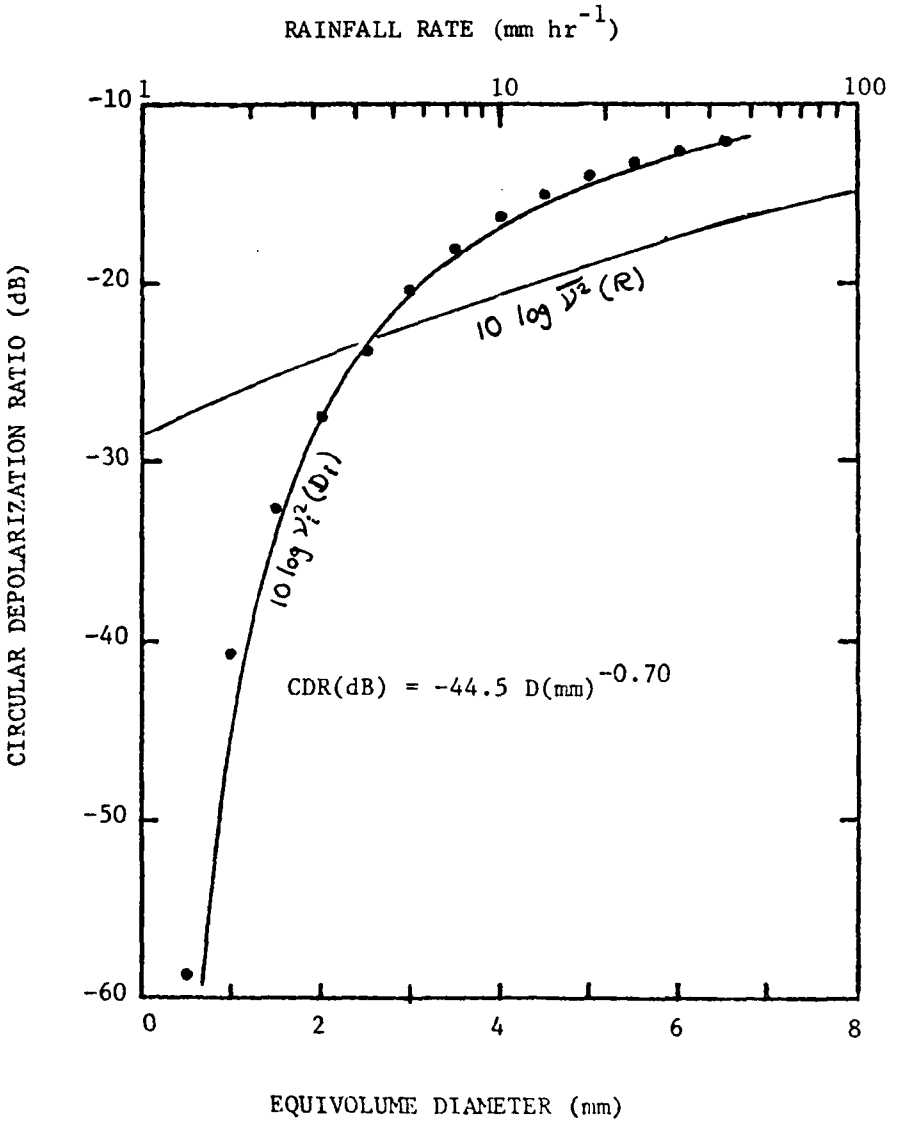

Figure 1. Circular depolarization ratio due to scattering, as a function of rainfall rate and of individual rain drop diameter. Values in rain are those of Humphries (4). Values due to individual drops are based on radar beam incidence perpendicular to the drop symmetry axis; points represent the calculations of McCormick and Hendry (1), and line corresponds to the model of Warner and Rogers (5).

A number density parameter can be obtained from the total backscatter reflectivity, once a drop size parameter is known, by means of the Rayleigh or Mie scattering cross section. If a drop size distribution is assumed to be describable by two parameters, e.g., an exponential function, then the measurements of total reflectivity plus depolarization ratio or of total reflectivity plus differential reflectivity (at two linear polarizations) can be used to define the distribution.

If Doppler frequency spectra of the received signals can be obtained from coherent radar data and if the Doppler frequency includes a substantial component due to raindrop fall speed, then the ratio of the power spectra of two circularly polarized backscatter components may be used to derive the drop shape as a function of Doppler frequency[2]. It has been suggested that spectra of signals measured at orthogonal linear polarizations should yield the same information as spectra derived from circularly polarized signals, but this has not been proven theoretically and probably requires pulse-to-pulse polarization agility.

Orientation parameters are derivable from the cross correlation or the cross spectrum of two circularly polarized backscatter components. The magnitude of the cross correlation of backscatter signals from rain is generally between 0.6 and 0.9, indicating that rain is a strongly oriented medium, and the phase of the cross correlation is near zero, indicating a mean canting angle near zero. We anticipate that some advantage will be gained from the spectral display of these parameters, i.e., through the cross spectrum, although the quantitative nature of the advantage is not known. Because the raindrop canting angle appears as an additive term with the non-Rayleigh differential phase shift in the exponent of the signal in the transmission channel, the availability of the cross spectrum should facilitate the identification of non-Rayleigh scattering effects in particular spectral bands.

Propagation effects are a key factor in system design, as they affect the maximum range of certain measurement capabilities. While total attenuation is important, as with single channel meteorological radars, differential attenuation and differential phase shift are even more important in the case of a dual-channel radar. These differential propagation terms are the differences of attenuation and of phase shift of signals propagating with polarizations parallel and perpendicular to the symmetry axis of the raindrops. In the context of dual-channel radar measurements, the propagation effects appear as a signal component in one channel due to scattering, absorption, or phase shift of the signal of the opposite polarization as it encounters non-spherical raindrops. Propagation effects are minimized for horizontal and vertical polarizations in rain because of the orientation of the propagation medium, but are non-zero because of the distribution of raindrop canting angles about the mean. Differential propagation effects are maximized for 45^{o} linear or for circular polarizations because the orientation of the polarization plane (in the linear case) or the circularity is altered by the non-spherical drops. For circular polarization, the major received signal has a sense of rotation opposite to the transmitted polarization and is generally 10 to 30 dB above the signal received in the transmission channel; therefore, the propagation component is included only in the transmission channel. Similarly, for linear polarization, the major received signal is parallel to the transmitted polarization; therefore, the propagation effect is included in the perpendicularly polarized component, since the propagation effect on the parallel polarized signal is negligible.

These characteristics of the propagation effects have led to the use or advocacy of linear or circular polarizations for various applications[3]. Although the minimizing of propagation effects makes linear polarization desirable or necessary for some purposes, the variety of measurement objectives we contemplate appears to require the use of circular polarization. Most of these objectives are related to the measurement of the anisotropy

of the scattering medium, and the measurements require circular polarization or pulse-to-pulse agile linear polarization. The increased propagation effects encountered with circular polarization can be viewed as an undesirable or detrimental factor in some situations, particularly for measurements of scattering parameters through precipitation, e.g., on the far side of a storm. Propagation effects that dominate the backscattering effects can provide valuable physical information about the propagation medium. For circular polarization, the formulation for the received signal in the transmission channel contains the factor

$$[\ \nu e^{j(\delta \pm 2\alpha)} + 2p\, e^{j(\chi \pm 2\tau)}\ ],$$

where ν is the amplitude ratio of the backscattered signals and p is related to the total one-way differential attenuation (ΔA) and differential phase shift ($\Delta\phi$) by the relation

$$p\, e^{j\chi} = \tanh\,(0.0575\Delta A + j\,(\pi/360)\Delta\phi). \qquad (1)$$

The relative significance of scattering and propagation effects can be determined from the quantity $2p/\nu$. Figure 2 illustrates the ranges at which propagation effects begin to be significant, as functions of rainfall rate and frequency. The propagation parameter (p) was derived from computations of Oguchi and Hosoya[6], and the amplitude ratio (ν) was derived from computations of Humphries[4]. Research aimed at separating propagation and scattering terms in the received signals is in progress[7].

6 Oguchi, T., and Hosoya, Y., 1974: Scattering Properties of Oblate Raindrops and Cross Polarization of Radio Waves Due to Rain (Part II): Calculations at Microwave and Millimeter Wave Regions. J. Radio Res. Labs. (Japan), 21, 191-259.

7 Metcalf, J. I., 1980: Propagation Effects on a Coherent Polarization-Diversity Radar. 19th Conf. Radar Meteor., Amer. Meteor. Soc.

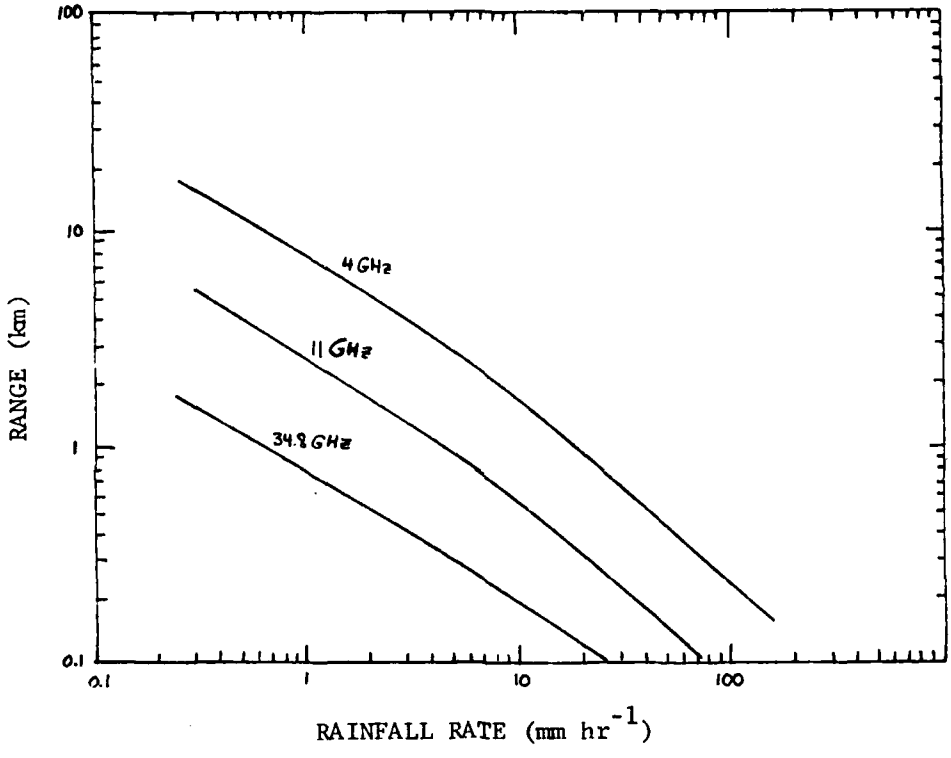

Figure 2. Relative significance of scattering and propagation terms in rain. Ranges for which $2p/\nu = 0.1$ are shown as functions of rainfall rate for frequencies of 4, 11, and 34.8 GHz.

B. SNOW

Within this designation, we include not only the relatively simple "single crystal" snow, but also more complicated "aggregate" snow and other ice forms such as sleet and graupel. One important objective of radar observations of snow is identification, i.e., detecting snow and discriminating it from rain. The extent to which this can be done varies widely according to the type of precipitation and other factors.

The shape of snowflakes should be measurable in the same ways as that of rain drops. In the case of snow, the electromagnetic shape may or may not be related to the physical shape, however, and neither is related to particle size in a well-defined way. Single crystal forms may have axial ratios between 0.1 and 10, but these rarely grow to precipitation size. Precipitating snowflakes tend to have more complicated shapes resulting from multiple crystal growth regimes or from aggregation. The circular depolarization ratio obtained from measurements of such particles at 16.5 GHz is usually small (i.e., large cancellation ratio), approaching -30 or -40 dB in some cases, and the circularly polarized backscatter component in the transmission channel is essentially unmeasurable in many situations with existing radar equipment.

Because snow particle shape is not related to size in a well-defined way, it is not possible to estimate particle sizes directly from shape measurements. Particle size will probably be most accurately estimated from measurements of the Doppler frequency shifts associated with their fall speeds. An ambiguous estimate of particle size and number density is obtainable from the total backscatter reflectivity, and it may be that the use of a coherent radar will permit a derivation of average particle size. It may be possible to determine number densities and particle sizes if models can be developed to relate these parameters to the total reflectivity and characteristics of the spectral functions.

It has been hypothesized that precipitating snow, unlike rain, is randomly oriented in space. One objective of measure-

ments of the type contemplated in this design project is to verify that this is so. Thus, the capability of deriving the complex cross spectrum from circularly polarized backscatter signals is essential, although the magnitude of the cross spectrum or the cross correlation is likely to be rather small (less than about 0.3). The cross correlation or cross spectrum may be useful for classifying ice precipitation in an empirical way. If snowflakes tend toward random orientation as hypothesized, they constitute an approximately isotropic propagation medium. Although signals of higher frequencies may be measurably attenuated in moderate to heavy snow, differential attenuation is expected to be small. Differential phase shift will also be small, except in conditions where the particles are strongly oriented by either aerodynamic forces (associated with crystal shape) or electric fields. Hence, the normalized quantities such as the circular depolarization ratio, spectral power ratio, cross correlation, and coherency spectrum will usually provide valid information on the scattering medium even at long ranges through snow, provided that the signal strength is sufficient.

C. HAIL

Identification of hail can be accomplished to some extent on the basis of reflectivity alone, since the highest observed meteorological reflectivities are almost always associated with large hail. The identification of small hail and the interpretation of cases in which reflectivity is near the "threshold" value for operational hail identification require the evaluation of other backscatter parameters. Great variation in reflectivity is observed, due to the variety of forms of hail, such as "spongy" ice or water-coated ice, and Mie scatter cross section variations with hailstone size. The effects of these variations on the polarization parameters is not known.

Hail at the surface is usually observed to be approximately spherical in shape, although irregularities and deviations are common. These irregularities give rise to significant depolarization of both linearly and circularly polarized signals. In the

case of circular polarization, circular depolarization ratios of -10 dB or greater (cancellation ratio of 10 dB or less) have been observed at 3 GHz. It has been hypothesized that hail aloft is sufficiently non-spherical to be affected by aerodynamic forces and thus to have a preferred orientation. If this be true, then hail shape could be derived from either circularly polarized signals in two receiver channels or from differential reflectivity measurements using linear polarization. Either of these measurements could be contaminated by differential attenuation, and differential phase shift could contaminate the circular polarization measurements even at 3 GHz. Such differential propagation effects are likely to be due to rain in the intervening medium.

The size of hailstones can probably be derived only from characteristics of Doppler spectral functions. Observations at 3 GHz indicate that hail is randomly oriented in space (contrary to the hypothesis mentioned above) and thus is characterized by low values of cross correlation or cross spectrum. If the presence of hail can be determined in a particular frequency band of the spectral functions, then the size of hail can be estimated from the corresponding fall speed. Fall speeds of hail, rain, and snow are shown in Figure 3. The use of Doppler frequency shift to derive hail size requires that measurements be made at a radar elevation angle sufficiently high that the Doppler component due to fall speed is measurable. This criterion is discussed further in Section III.

Number density of hail can be determined from the total backscatter intensity, provided that hail size is determined first. Otherwise, the size and number density are ambiguously related. The use of two microwave frequencies (e.g., 3 and 6 GHz) to measure the frequency dependence of the total backscatter has resulted in some success in identifying hail and in determining its size and number density.

The spatial orientation of hail is of interest for several reasons, and, as implied above, disagreement exists as to whether hailstones are or are not preferentially oriented. Methods

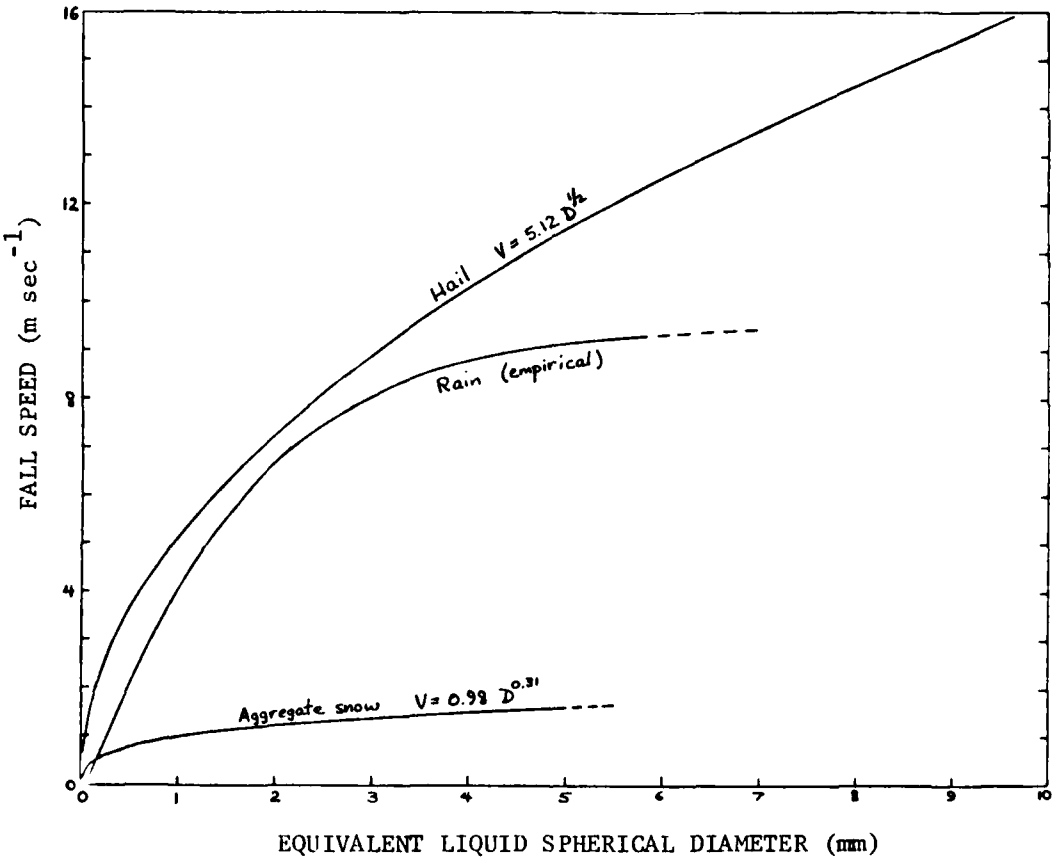

Figure 3. Fall speeds of rain, hail, and snow as functions of hydrometeor size.

similar to those employed for rain can be used to measure the orientation of hail. Parameters that seem best suited for deriving the spatial orientation of hail are either the magnitude and phase of the cross correlation of the spectral coherency and phase computed from the two circularly polarized backscatter components.

Significant attenuation can occur if hail is present, due to both the hail itself and heavy rain in the vicinity. Differential propagation effects are also likely to be large, leading to depolarization of either linearly or circularly polarized signals which can be measurable even at 3 GHz. The cross correlation of circularly polarized signals may provide valuable information in such situations since differential propagation effects appear as an increasing magnitude of cross correlation with range. Large values of circular depolarization ratio can be interpreted as due to hail backscatter if the cross correlation is small. If the cross correlation or coherency is large, then the corresponding large values of depolarization must be due either to propagation effects or to oriented scatterers.

D. LIQUID WATER CLOUD

The distinction between precipitating and non-precipitating water particles is somewhat arbitrary, given that fall speed is a continuous monotonic function of drop size. The dividing point is usually taken about 200μm diameter, where terminal fall speed is about 0.8 m sec^{-1}. Weak vertical motions which are present even in clouds of small vertical extent are sufficient to keep these particles suspended indefinitely.

Because so-called cloud water drops are nearly spherical in shape, they may be expected to produce negligible depolarization. This criterion together with the measurement of reflectivity may therefore be used to identify liquid water clouds. The formation of precipitation should be accompanied by a gradual increase of depolarization as well as a rapid increase in reflectivity. The depolarization ratio may be used in conjunction with the reflectivity and cross correlation to document the formation

of precipitation and to distinguish between depolarization due to rain and due to ice crystals.

Reflectivity of clouds has been found to be approximately proportional to the square of the liquid water content[8]. This result implies that the size distribution of water drops in clouds is relatively narrow, since the proportionality would be exact if all the drops were of equal size. Water content of various types of clouds ranges from less than 0.1 gm m^{-3} to several grams per meter cubed. Typical reflectivities at microwave frequencies are shown in Figure 4.

Since depolarization is negligible, both in scattering and in propagation, across the entire microwave region, only the power spectrum of the signal in the "main" channel (i.e., the channel opposite to the transmission channel in the case of circular polarization) will contain useful information. Specifically, mean velocity and spectrum width provide information on the large and small scale variations of air velocity in the cloud. In cases where the presence of ice crystals is suspected (or cannot be ruled out on the basis of temperature) or where the development of precipitation is anticipted, the other spectral functions should be available from the radar data.

E. ICE CRYSTAL CLOUDS

Ice crystals of non-precipitating size represent what is perhaps the least documented class of meteorological scattering media. Because they occur both in thin high-altitude clouds and in the upper regions of clouds producing rain, the development of techniques and equipment for observing them involves consideration both of the scattering and propagation characteristics of the ice crystals themselves and of the propagation characteristics of other hydrometeor types.

The presence of ice crystals in clouds may be determined by the joint use of radar reflectivity (typically lower than in

[8] Battan, L. J., 1973: Radar Observation of the Atmosphere. University of Chicago Press.

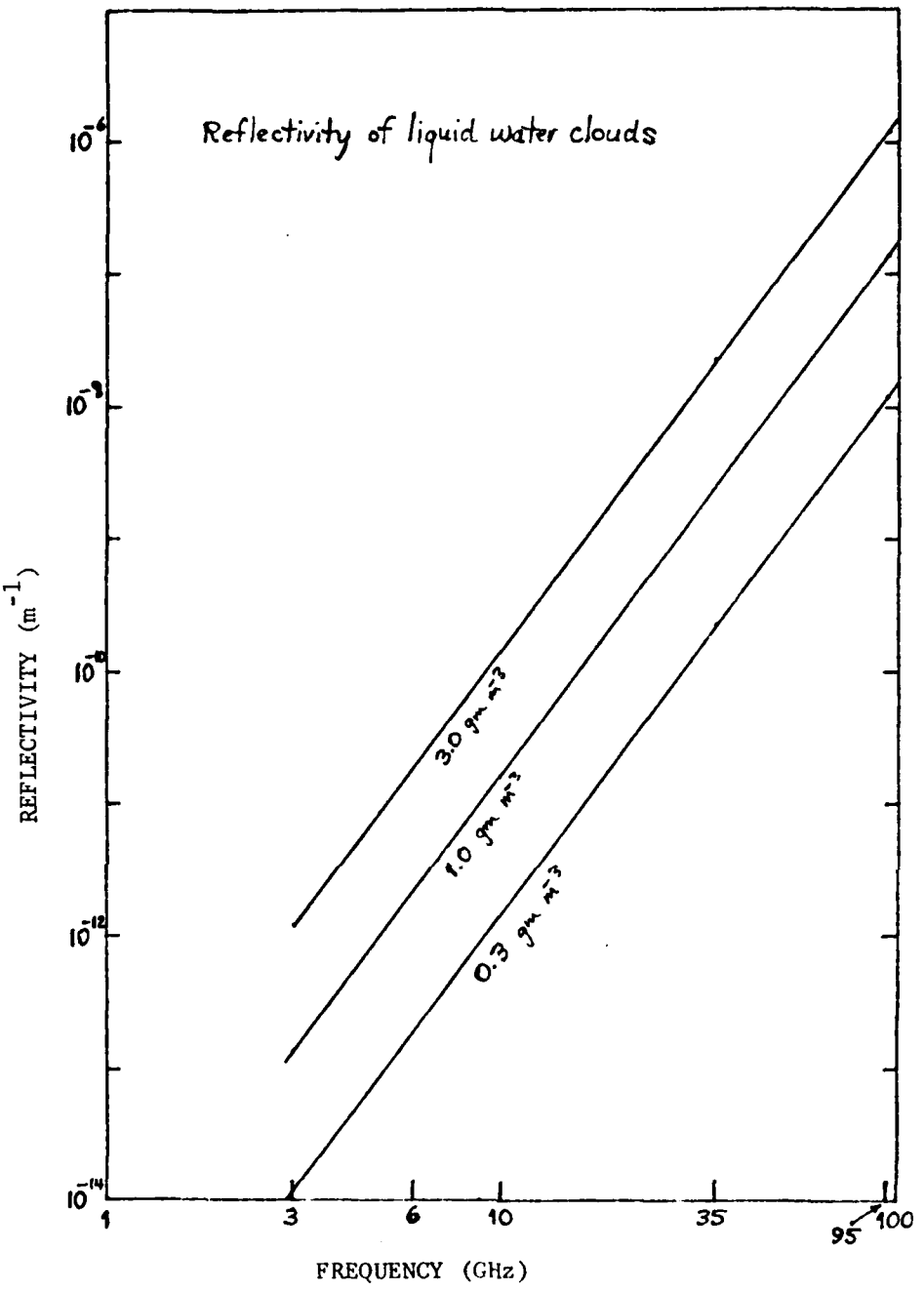

Figure 4. Reflectivity of liquid water clouds as a function of radar frequency for typical values of water content.

liquid water clouds), depolarization ratio (non-zero for sufficiently non-spherical crystals), orientation parameters, and in some cases propagation parameters. Reflectivity of ice crystal clouds is approximately proportional to the square of the water content, but is about 6.7 dB less than that for liquid water clouds of similar water content because of the different dielectric factor for ice. A wide range of depolarization ratios are possible as a result of the various shapes of ice crystals. Calculations of backscattering from ice ellipsoids yield circular depolarization ratios as large as -7.5 dB for preferentially oriented scatterers with an axis-to-diameter ratio of 0.1.

Because of the extreme values of axis-to-diameter ratios which ice crystals may attain, relative to those of raindrops, significant differential propagation effects may occur. This is particularly true if the crystals are preferentially oriented by aerodynamic or electrical forces. Such effects have been observed in radar backscatter at 16.5 GHz and in satellite-to-ground communications at 20 GHz. The propagation effects observed by radar were believed to be due to ice crystals too small to be detectable; detectable backscatter from greater range revealed the propagation effects in the intervening space. Differential phase shift up to 2.5 deg km^{-1} was calculated from these observations; differential attenuation was negligibly small. With the differential attenuation so small, transmission on only one circular polarization is required to obtain the orientation angle of the propagation medium (from the phase of the cross correlation between the two circularly polarized received signals), if propagation effects are dominant. Polarization switching will be necessary to fully document situations in which scattering and propagation effects are of comparable magnitudes.

SECTION III
RADAR SYSTEM ANALYSIS

A radar system analysis was performed to determine the optimum transmitting frequency and other radar parameters for the various measurement scenarios. The only system attributes assumed a priori were coherence and polarization diversity. The optimum radar system configuration for a given meteorological measurement depends on the measurement scenario, including target type (rain, snow, hail, clouds), propagation medium (clear air, rain-filled), target range, and target elevation angle. The most important radar parameter to be determined is the radar operating frequency, which is extremely dependent on the measurement scenario. For example, raindrop shape measurements at long range through a rain-filled propagation medium dictate a radar operating frequency in S-band, not only to minimize attenuation due to propagation so that the rain in the resolution cell can be detected, but also to minimize depolarizaton due to propagation so that raindrop shape can be accurately measured. However, measurements of water and/or ice clouds through a clear air propagation medium necessitate a higher radar frequency, say K_a-band, so that detection can occur. No one single-band radar system will be optimum for all meteorological measurements of interest.

Target ranges and elevation angles are considered in general in Subsection A. Also considered are ambiguity trade-offs between maximum unambiguous range and maximum unambiguous Doppler frequency. Design considerations affecting detection of the various meteorological targets are discussed in Subsection B, and polarization factors influencing radar design are considered in Subsection C. The utility of multiple-frequency observations and frequency modulation techniques is discussed in Subsection D. The results of the analysis are summarized in Subsection E.

A. COVERAGE

The selection of area coverage for the radar is determined primarily by desired measurements of target characteristics and secondarily by hardware/component limitations. Because clouds and precipitation occur within the troposphere, we selected a nominal maximum altitude of 14 km for analysis of the radar scanning geometry. For a measurement radar located on the surface of the earth, the geometry is depicted in Figure 5. The maximum range (using a 4/3 earth approximation) is a function of the elevation angle, given the 14 km altitude limit, and is graphed in Figure 6. Here we see a rapid increase in range at angles less than about 6 degrees. The fall speeds for the targets of interest are indicated in Figure 3. (Cloud particles have fall speeds less than about 0.5 m sec^{-1}.) The velocity component along the radar-line-of-sight (RLOS) determines the observed Doppler frequency of the target. For vertically falling targets (towards center of earth) the velocity components along the RLOS is proportional to the sine of the elevation angle at which the target is observed. Since Doppler frequency is related to the velocity by

$$f_d = 2 V_{RLOS}/\lambda = 2V_f \sin\phi/\lambda \qquad (2)$$

the Doppler frequency increases with increasing elevation angle and with decreasing radar wavelength. For target classification purposes, it is desirable to obtain as much spread in Doppler as possible. Thus, high elevation angles and/or high frequencies (short wavelengths) are advantageous.

Slower fall-speeds are mostly associated with smaller particles and correspondingly lower reflectivity. Many target data processing applications require both received polarizations to be measured with significantly high signal-to-noise ratios (SNR). This leads to a higher transmitted power requirement or reduced range capability.

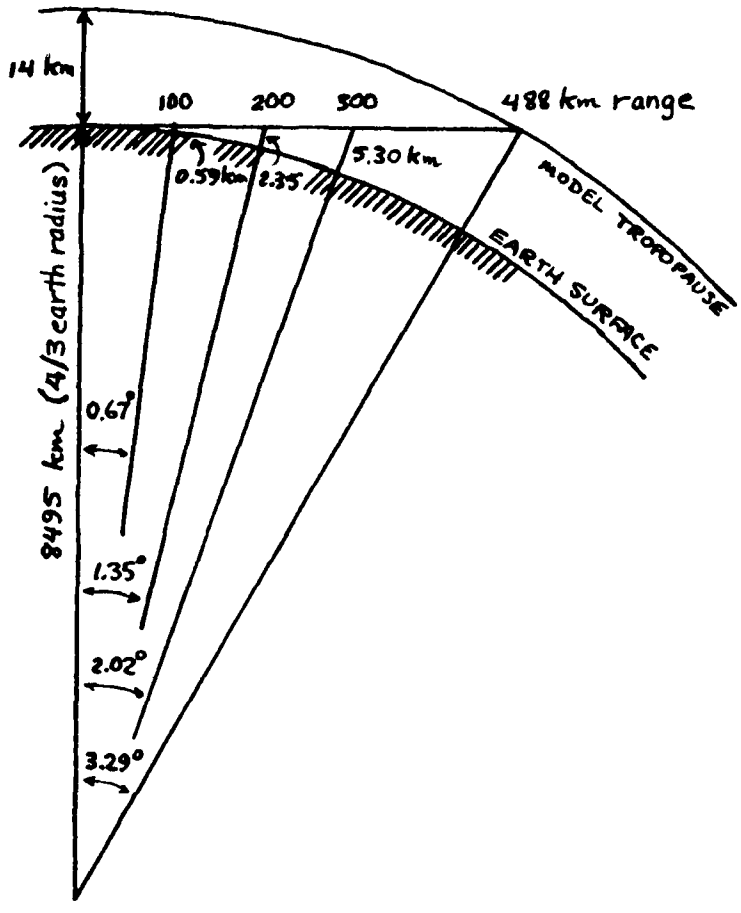

Figure 5. Scanning geometry (based on 4/3 earth radius).

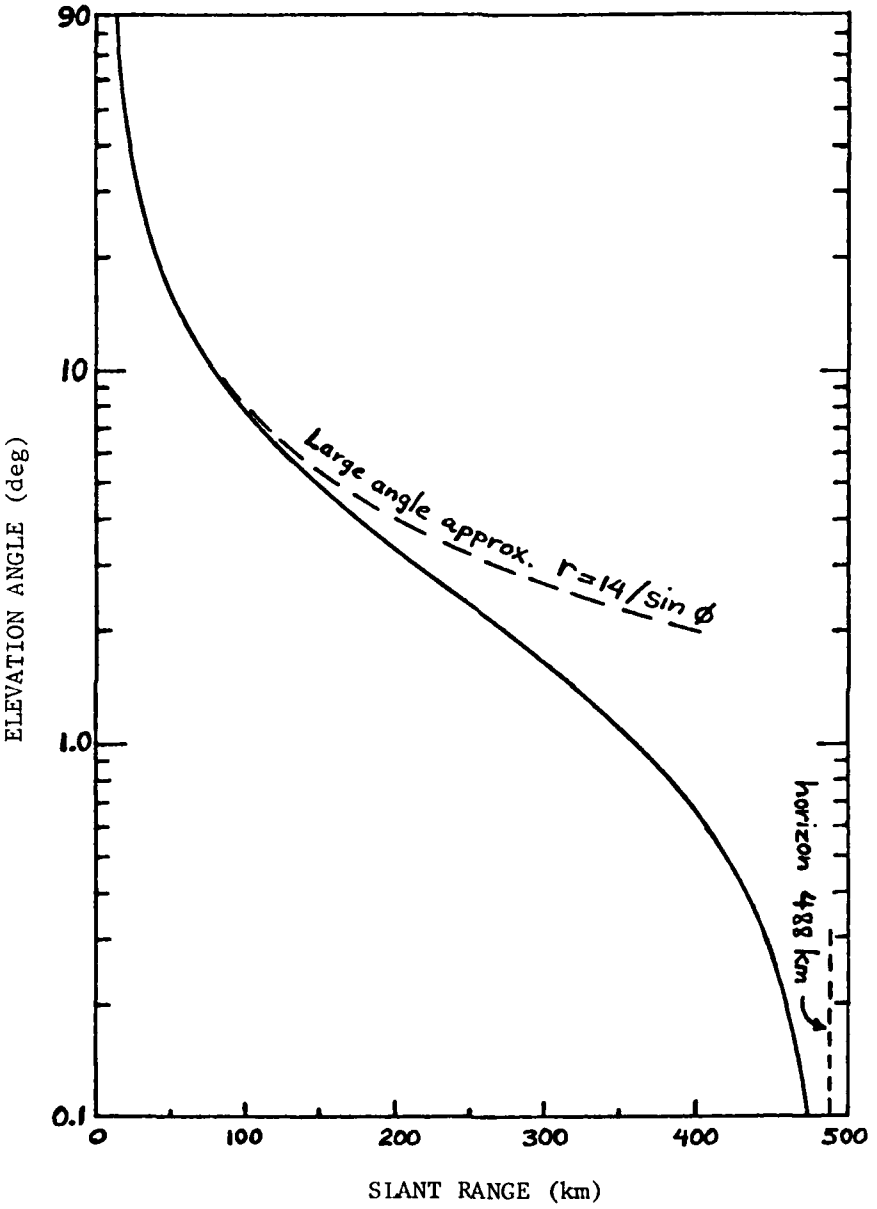

Figure 6. Elevation angle as a function of slant range to the tropopause (assumed at 14 km altitude).

An additional constraint on the measurement capability is introduced by the angular dependence of depolarization in the anisotropic scattering medium. This angular dependence is best illustrated by rain, since the raindrops fall as oblate spheroids. Depolarization due to rain will be largest when rain is viewed at horizontal incidence and near zero when viewed vertically. The power ratio for circularly polarized signals backscattered from rain varies as the fourth power of the cosine of the elevation angle. The angular dependence of depolarization and the angular dependence of the Doppler frequency due to fall speed (Equation 2) are shown in Figure 7. This figure implies that analyses dependent on having both a mesurable Doppler frequency component due to fall speed and a measurable depolarization ratio are restricted to elevation angles between about 15 and 45 degrees.

The optimum coverage areas for the desired target measurements are also limited by a combinaton of range and power constraints. Optimum coverage parameters are summarized in Table 1. The remainder of the radar system analysis was based on providing primary area coverage. Measurements at lower elevation angles and greater ranges will be possible within the constraints of propagation effects and an increasing spatial resolution increment. However, the capability to make all desired measurements at long range will be limited.

Range and Doppler ambiguities are to be avoided or a method for resolving them must be incorporated into the radar design. Under the assumption of the 14 km altitude maximum, the maximum range to the targets as a function of elevation angle was given in Figure 6 versus elevation angle. The radar Pulse Repetition Frequency (PRF) required to maintain unambiguous range information is governed by the relation

$$PRF \leq c/2r(\phi)$$

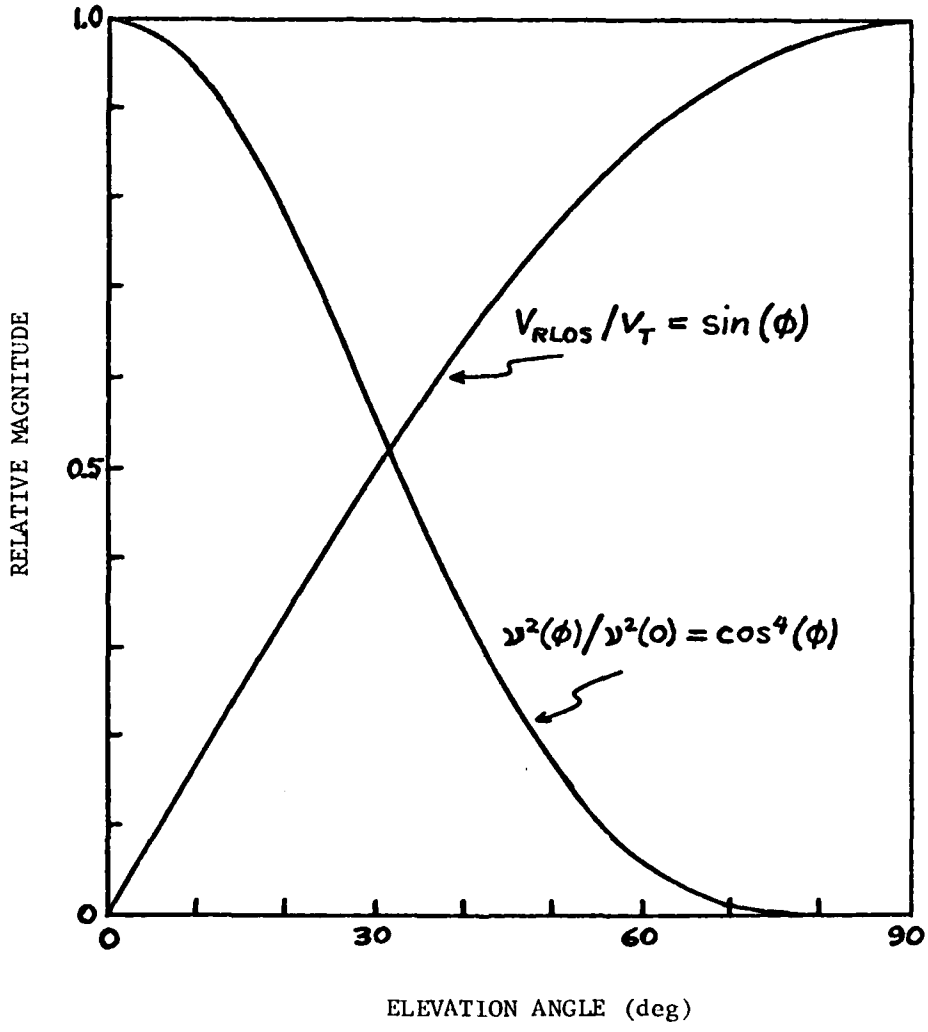

Figure 7. Relative target velocity along radar line of sight (RLOS) due to fall speed, and relative circular polarization power ratio (circular depolarization ratio) in rain, as functions of radar elevation angle.

TABLE 1. SUMMARY OF COVERAGE

PARAMETER	COVERAGE
Primary Region	
Azimuth	0^{o} - 360^{o}
Elevation	15^{o} - 90^{o}
Range	0 - 40 km
Doppler Velocity	<20 m sec^{-1}
Secondary Region	
Azimuth	0^{o} - 360^{o}
Elevation	0 - 15^{o}
Range	0 - 200 km
Doppler Velocity	<20 m sec^{-1}

where c is the velocity of light (3×10^8 m sec^{-1}) and $r(\phi)$ is the range of interest. Figure 8 illustrates the PRF constraints as a function of elevation angle. At the horizon the PRF is constrained to be less than 307 Hz, while above 50 degrees elevation PRF can exceed 10,000 Hz. The radar designs in the following sections accommodate this wide range of values.

For unambiguous Doppler measurements, the PRF must be at least twice the maximum Doppler frequency. Using the PRF constraint versus elevation from Figure 8,

$$PRF(\phi) \geq 2f_d = 2\,[2\,V_{RLOS}/\lambda] = 4\,V_{RLOS}\,f_o/c \qquad (3)$$

Solving for frequency, f_o, we obtain

$$f_o \leq c\,PRF(\phi)/(4\,V_{RLOS}/\lambda) \qquad (4)$$

Figure 9 shows this result for various values of V_{RLOS}. For the primary measurement area of 40 km range and a nominal minimum elevation angle of 15 degrees, the frequencies of the radar should be less than 56, 26, and 13 GHz for line-of-sight velocities of 5, 10, and 20 m sec^{-1}, respectively. It must be remembered that V_{RLOS} incorporates the components of velocity due to the fall speed and horizontal wind, and applications of the frequency constraint curves should account for expected velocities along the radar-line-of-sight, not necessarily absolute maximums.

B. DETECTION

Target detectability is a basic criterion for meteorological radar measurements. Target detection depends on the target radar cross section (RCS), radar characteristics such as transmitting frequency, peak power, pulse width, beamwidth, etc., and propagation effects. Of the meteorological targets and propagation media under consideration, only rain is amenable to an analytical

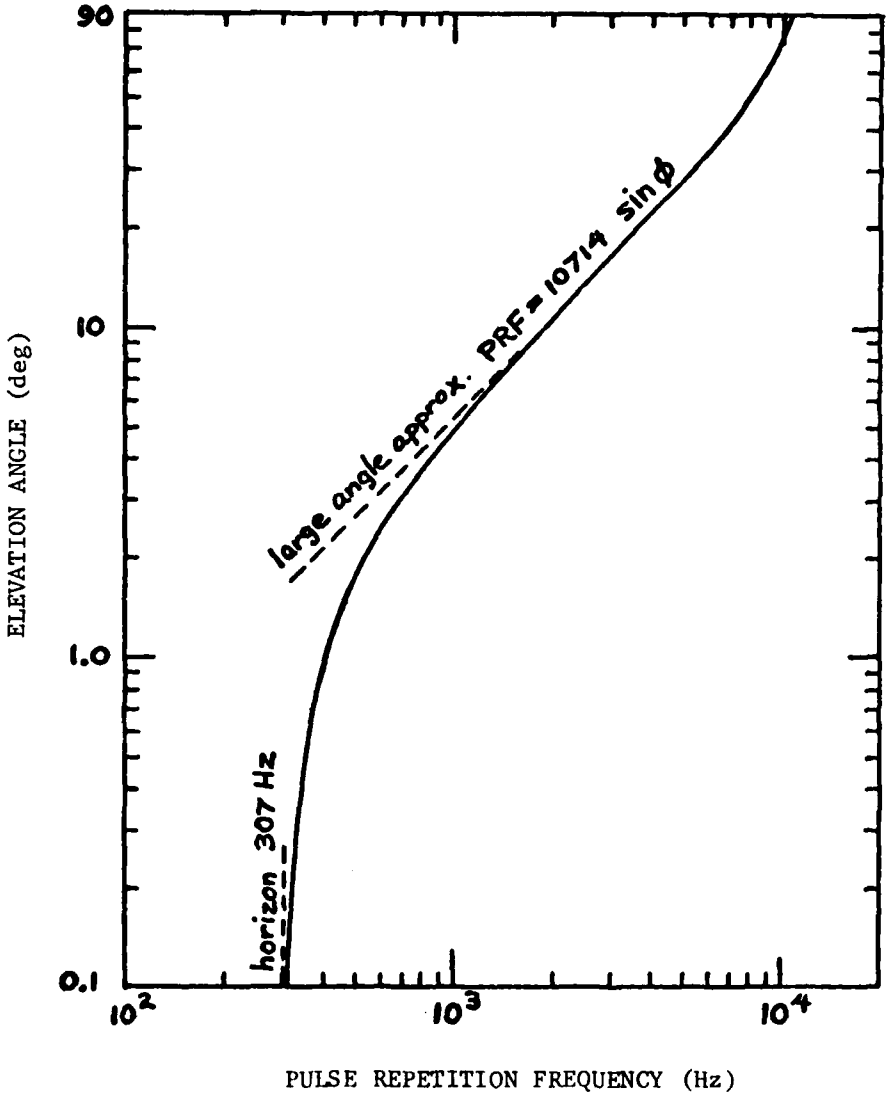

Figure 8. Maximum pulse repetition frequency for unambiguous range measurement, as a function of elevation angle.

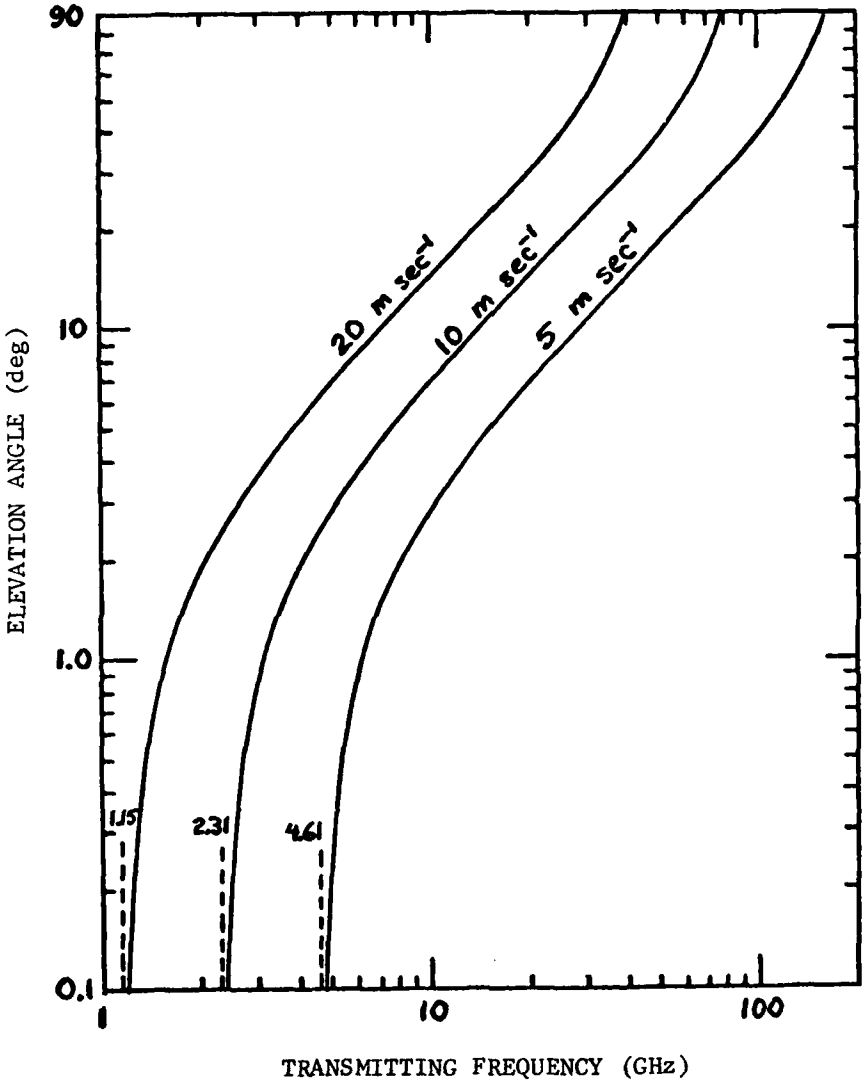

Figure 9. Maximum radar transmitting frequency as a function of elevation angle, for unambiguous range measurement and unambiguous Doppler velocity limits shown. Acceptable frequencies are to the left of the plotted curves.

expression for RCS. Hence, the following discussion relates primarily to rain and secondarily to other target types.

For simplicity, detection criteria for rain was based on a spherical raindrop model. The RCS for a single spherical raindrop, assuming Rayleigh scattering ($D<<\lambda$), is given by

$$\sigma = (\pi^5/\lambda^4) |K|^2 D^6 \tag{5}$$

where $K = (\varepsilon - 1)/(\varepsilon + 2)$, λ is the transmitted wavelength, D is the diameter of the raindrop, and ε is the complex dielectric constant of water. Although ε varies greatly over radar operating frequencies, $|K|^2$ remains relatively constant and is numerically equal to approximately 0.93. The total RCS for a large group of spherical raindrops in the resolution volume (cell) of the radar is determined by summing the RCS of raindrops in that volume. The reflectivity (η) is defined as the total RCS per unit volume and is related to the reflectivity factor Z by the relation

$$\eta = \frac{\pi^5}{\lambda^4} |K|^2 Z \times 10^{-10} \tag{6}$$

where λ is given in centimeters and Z in the customary units of mm^6m^{-3}. For a Marshall-Palmer[9] raindrop size distribution, reflectivity is given by

$$\eta = (2 \times 10^{-8}) \pi^5 |K|^2 R^{1.6} \lambda^{-4} \tag{7}$$

where η is reflectivity (m^{-1}), R is rainfall rate (mm hr^{-1}), λ is wavelength (cm).

A graph of η versus frequency, $f = c/\lambda$, is shown in Figure

[9] Marshall, J. S., and Palmer, W. M., 1948: The Distribution of Raindrops With Size. J. Meteor., 5, 165-166.

10 for rain rates of 1, 5, 10, and 50 mm hr^{-1}. The solid lines in Figure 10 indicate the range in which the Rayleigh approximation to the backscatter is valid. The broken lines are continuations of the Rayleigh scattering approximation into regions where Mie scattering effects can generally not be neglected. Also plotted are the values of η for the various rain rates at f = 16, 24.2, and 35 GHz; these points are based on Z-R relationships calculated by Wexler and Atlas[10], which were based on Mie backscattering cross sections. As expected, the Rayleigh scattering approximation is poorest at large rain rates (large drop sizes) and high frequencies (short λ).

An analysis of snow reflectivity is not possible due to the irregularity of the size and shape of snowflakes. However, from various snowfall measurements, the following empirical relation has emerged:

$$\eta = (2 \times 10^{-7}) \pi^5 |K|^2 R^2 \lambda^{-4} \qquad (8)$$

where R (mm hr^{-1}) is the precipitation rate when the snow has melted and λ is in centimeters. The dielectric factor $|K|^2$ now has an approximate value of 0.197. A plot of η versus f is shown in Figure 11 for precipitation rates of 1, 5, 10, 15, and 20 mm hr^{-1}. Note that snow reflectivity is greater than rain reflectivity for all but the negligible precipitation rates; this is because snow falls much slower than rain, and the number density of snowflakes must be greater than that of rain drops to achieve an equivalent precipitation rate.

Reflectivity factors as high as $Z = 4 \times 10^6$ mm^6 m^{-3} have been observed for hail in thunderstorms. This corresponds to a reflectivity of $\eta = 3 \times 10^{-4}$ m^{-1}, or -35 dB, at X-band. Douglas[11]

[10] Wexler, R., and Atlas, D., 1963: Radar Reflectivity and Attenuation of Rain. J. Appl. Meteor., 2, 276-280.

[11] Douglas, R. H., 1964: Hail Size Distribution. Proc. 11th Wea. Radar Conf., Amer. Meteor. Soc., 146-149.

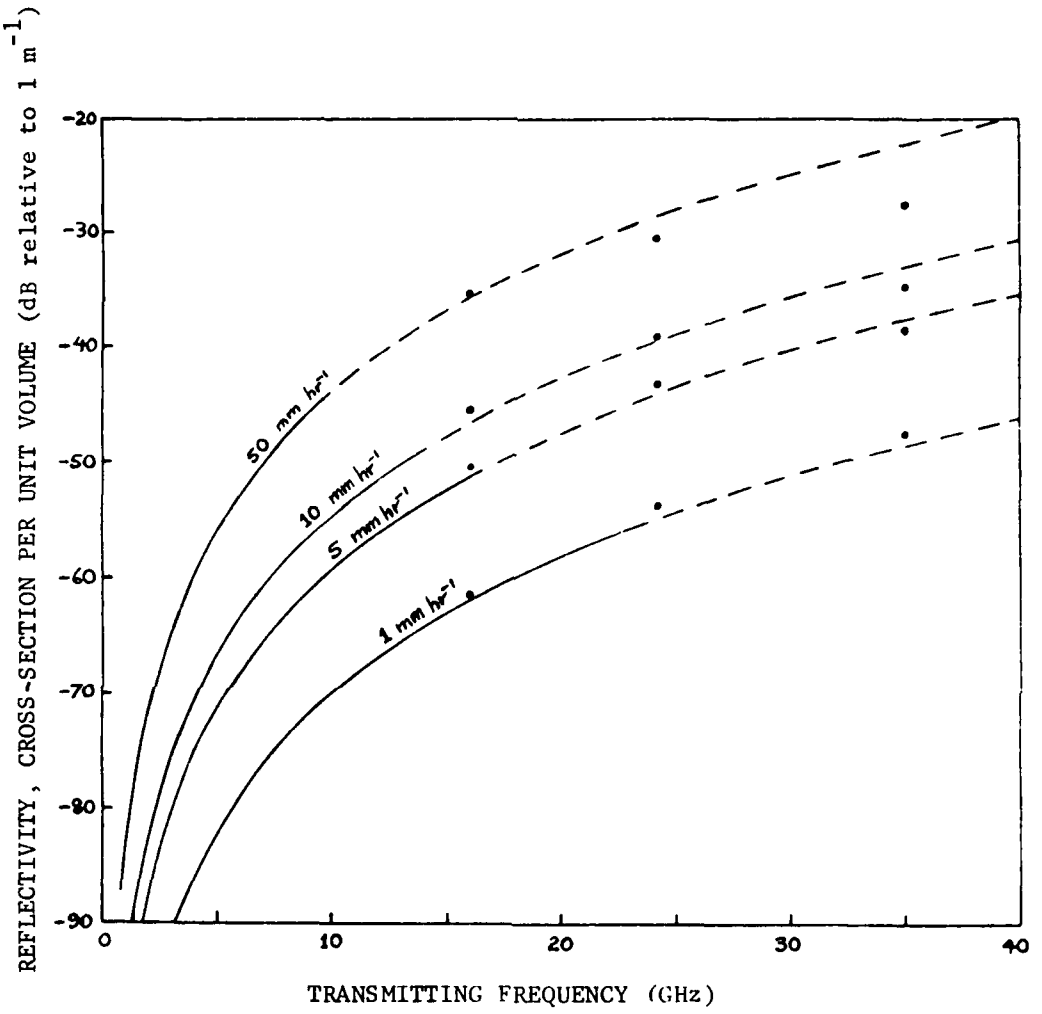

Figure 10. Reflectivity of rain. Solid lines represent Rayleigh scattering approximation over its range of validity. Broken lines are extrapolations of Rayleigh approximation to higher frequencies. Dots are calculated for Mie scattering.

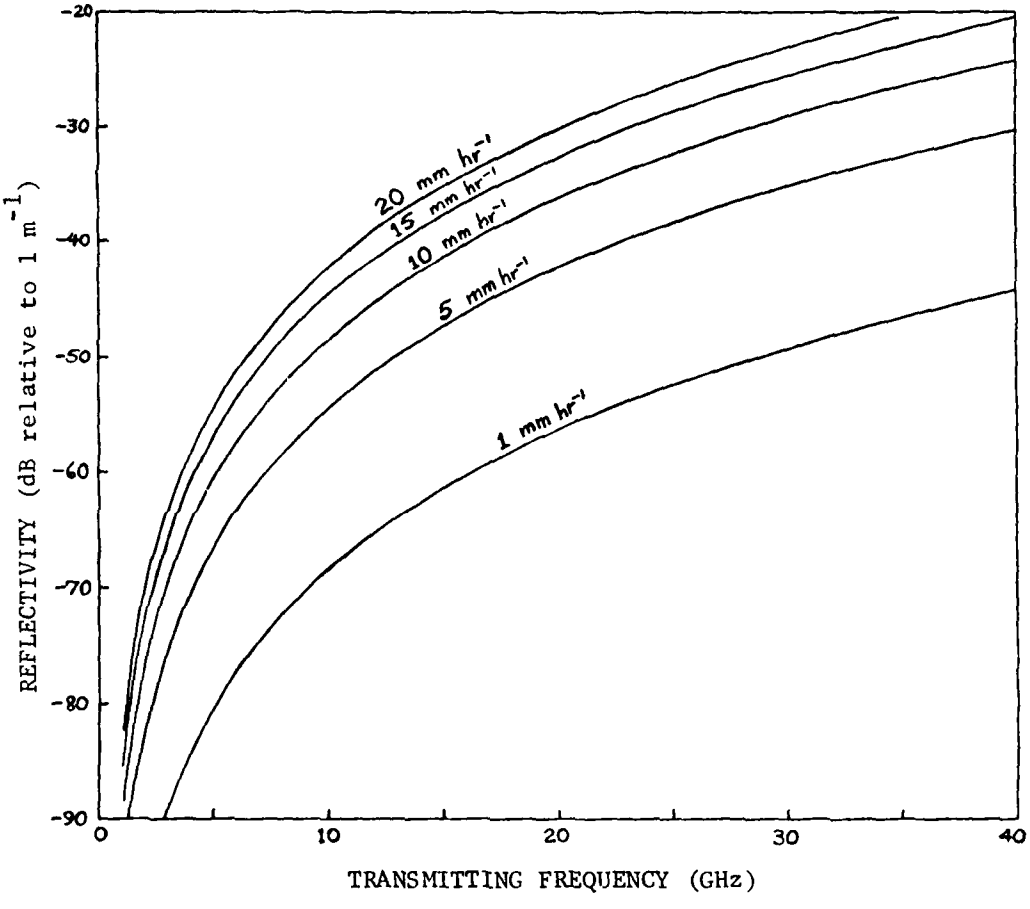

Figure 11. Reflectivity of snow, based on Rayleigh scattering.

found that for wet hail,

$$Z = 16000R^{0.97} \text{ mm}^6\text{m}^{-3} \text{ for } f = 9.1 \text{ GHz} \quad (9)$$

$$Z = 42000R^{0.96} \text{ mm}^6\text{m}^{-3} \text{ for } f = 3 \text{ GHz} \quad (10)$$

and for dry hail,

$$Z = 4200R^{0.97} \text{ mm}^6\text{m}^{-3} \text{ for } f = 9.1 \text{ GHz} \quad (11)$$

$$Z = 11000R^{0.97} \text{ mm}^6\text{m}^{-3} \text{ for } f = 3 \text{ GHz} \quad (12)$$

Using the value 10^4 as a representative value for the coefficient of R, we obtain

$$\eta = 10^{-6} \pi^5 |K|^2 R^{0.97} \lambda^{-4} \quad (13)$$

where R (mm hr^{-1}) is the precipitation rate when the hail has melted and λ is in centimeters.

Atlas[12] found for clouds,

$$\eta = (4.8\times10^{-12}) \pi^5 |K|^2 M^2 \lambda^{-4} \quad (14)$$

where M is water content in grams per meter cubed and $|K|^2 = 0.93$ for water clouds and 0.197 for ice clouds.

We can summarize the foregoing results for the assumed Rayleigh scattering with the relation

$$\eta = A \lambda^{-4}(m^{-1}) \quad (15)$$

where:

[12] Atlas, D., 1954: The Estimation of Cloud Parameters By Radar. J. Meteor., 11, 309-317.

$$A = (2\times10^{-8})\ \pi^5\ |K|^2\ R^{1.6} = 5.69\times10^{-6} R^{1.6} \qquad \text{for rain}$$

$$A = (2\times10^{-7})\ \pi^5\ |K|^2\ R^2 = 1.21\times10^{-5} R^2 \qquad \text{for snow}$$

$$A = 10^{-6}\ \pi^5\ |K|^2\ R^{0.97} = 6.03\times10^{-5} R^{0.97} \qquad \text{for hail}$$

$$A = (4.8\times10^{-12})\ \pi^5\ |K|^2\ M^2 = \begin{cases} 1.37\times10^{-9} M^2 & \text{for water clouds} \\ 2.89\times10^{-10} M^2 & \text{for ice clouds} \end{cases}$$

λ is in centimeters,

R is in millimeters per hour, and

M is in grams per meter cubed.

The radar equation, which gives the signal-to-noise ratio (SNR) as a function of radar and target parameters, must be considered to determine the values of the transmitting frequency and other radar parameters that maximize the probability of detecting hydrometeor targets. The single pulse SNR for a radar detecting a hydrometeor target is

$$SNR = \frac{10^{-4} P_t G^2 \eta V \lambda^2}{(4\pi)^3 F k T B r^4 L_s L_p} \qquad (16)$$

where:

P_t = peak transmitted power

G = antenna gain = $\pi^2/(\theta_{el}\ \theta_{az})$

η = reflectivity

V = volume of resolution cell = $(\pi/4) r^2\ \theta_{el} \theta_{az}\ (c\tau/2)$

λ = transmitted wavelength
r = range
c = speed of light
τ = pulse width
θ_{el} = elevation beamwidth (radians)
θ_{az} = azimuth beamwidth (radians)
F = noise figure
k = Boltzmann's constant
T = temperature
B = receiver bandwidth $= \tau^{-1}$
L_s = total system losses
L_p = total propagation losses

λ is in centimeters and all other quantities are in the MKS system of units

Propagation losses can be written as

$$L_p = e^{0.46\gamma(\lambda)r} \tag{17}$$

where $\gamma(\lambda)$ is the one-way loss (coefficient of attenuation) in decibels per unit length.

Consideration is now given to the frequency dependence of the SNR. Besides the explicit dependence of the SNR on λ^2, it also depends implicitly on λ through its dependence on η and $\gamma(\lambda)$. Wavelength can have a second order effect through its possible influence on P_t, F, and L_s, but these effects will be ignored here. The SNR can be divided into a λ-dependent factor and a λ-independent factor,

$$SNR = K\lambda^{-2}e^{0.4\gamma(\lambda)r} \tag{18}$$

The λ-independent factor K (not to be confused with the dielectric factor in the reflectivity formulations) is given by

$$K = \frac{10^{-4}\pi^2 P_t \tau^2 Ac}{512\ \theta_{el}\theta_{az}FkTr^2L_s} \tag{19}$$

or

$$SNR/K(dB) = -2\,\gamma(\lambda)r - 20 \log \lambda \qquad (20)$$

Antenna parameters are assumed to be varied with λ in such a manner as to render θ_{el} and θ_{az} constant and independent of λ .

The propagation medium must now be specified to proceed further. Two scenarios are investigated: a clear air, high humidity propagation medium, and a rain-filled propagation medium. The coefficient of attenuation, $\gamma(\lambda)$, can be written as

$$\gamma(\lambda) = \gamma_G(\lambda) + \gamma_R(\lambda) \qquad (21)$$

where $\gamma_G(\lambda)$ is due to absorption of radiation by gaseous oxygen and water, and $\gamma_R(\lambda)$ is due to attenuation of radiation by rain present in the propagation medium. In a clear air medium, $\gamma_R(\lambda)=0$, and Van Vleck[13] has shown that $\gamma_G(\lambda)$ in dB km^{-1} is given by

$$\gamma_G(\lambda) = \lambda^{-2}\left\{0.34\left[\frac{\Delta\nu_1}{\lambda^{-2}+\Delta\nu_1^2} + \frac{\Delta\nu_2}{(2+\lambda^{-1})^2+\Delta\nu_2^2} + \frac{\Delta\nu_2}{(2-\lambda^{-1})^2+\Delta\nu_2^2}\right]\right.$$

$$\left. + 0.0035\,\rho\left[\frac{\Delta\nu_3}{(\lambda^{-1}-0.741)^2+\Delta\nu_3^2} + \frac{\Delta\nu_3}{(\lambda^{-1}+0.741)^2+\Delta\nu_3^2}\right]\right\} \qquad (22)$$

where $\Delta\nu_1 = 0.018$, $\Delta\nu_2 = 0.049$, $\Delta\nu_3 = 0.087$, λ is in centimeters, and ρ is the absolute humidity. A graph of $\gamma_G(\lambda)$ versus λ is

[13] Van Vleck, J. H., 1947: Absorption of Microwaves by Oxygen and The Absorption of Microwaves by Uncondensed Water Vapor. Phys. Rev., 71, 425-433.

shown in Figure 12 for $\rho = 20$ gm m^{-3} (saturated air at ordinary temperatures).

For $\gamma(\lambda) = \gamma_G(\lambda)$, graphs of SNR/K(dB) versus λ for a clear air medium are shown in Figure 13 for r = 1,10,40, and 100 km. The peaks in the SNR/K vs. λ curves occur at values of λ that depend on range. The values of λ for which these peaks occur, for $\lambda > 0.5$ cm, are given in Table 2.

In the primary region of coverage (as defined in Subsection A) where target ranges vary from 0 to 40 km, the first maximum in a given SNR/K vs. λ curve is always greater than the second maximum. Thus, in this region, the transmitting frequency that maximizes the probability of detection of meteorological targets in a clear air propagation scenario is in the low millimeter wave band, or K_a-band. The next optimum operation frequency is in K_u-band or X-band.

TABLE 2. WAVELENGTH AND FREQUENCY FOR WHICH NORMALIZED SIGNAL TO NOISE RATIO IS MAXIMUM (PROPAGATION THROUGH CLEAR AIR)

r(km)	First SNR/K Maximum	Second SNR/K Maximum
1	0.60 cm (50 GHz)	
10	0.75 cm (40 GHz)	1.85 cm (16.2 GHz)
40	0.80 cm (38 GHz)	2.10 cm (14.3 GHz)
100	0.85 cm (35 GHz)	2.50 cm (12.0 GHz)

The coefficient of attenuation is given by Equation (21) if the propagation medium is rain-filled; i.e., $\gamma_R(\lambda)$ must now be included in $\gamma(\lambda)$. Burrows and Atwood[14] have given values for $\gamma_R(\lambda)$ for various rain rates and transmitting frequencies.

[14] Burrows, C. R., and Atwood, S. S., 1949: Radio Wave Propagation, Consolidated Summary Technical Report of the Committee on Propagation, NDRC, Academic Press, New York.

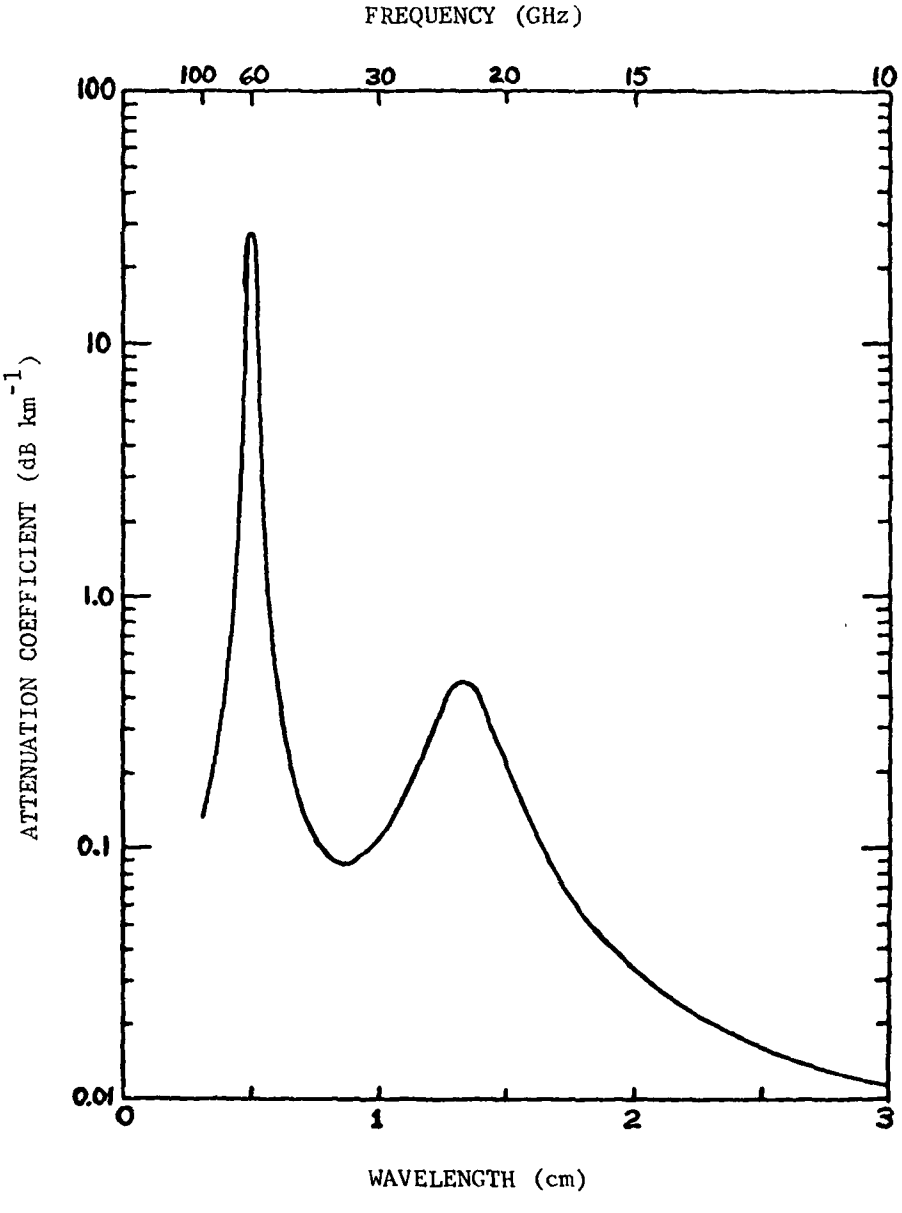

Figure 12. Attenuation coefficient for absorption by oxygen and water vapor.

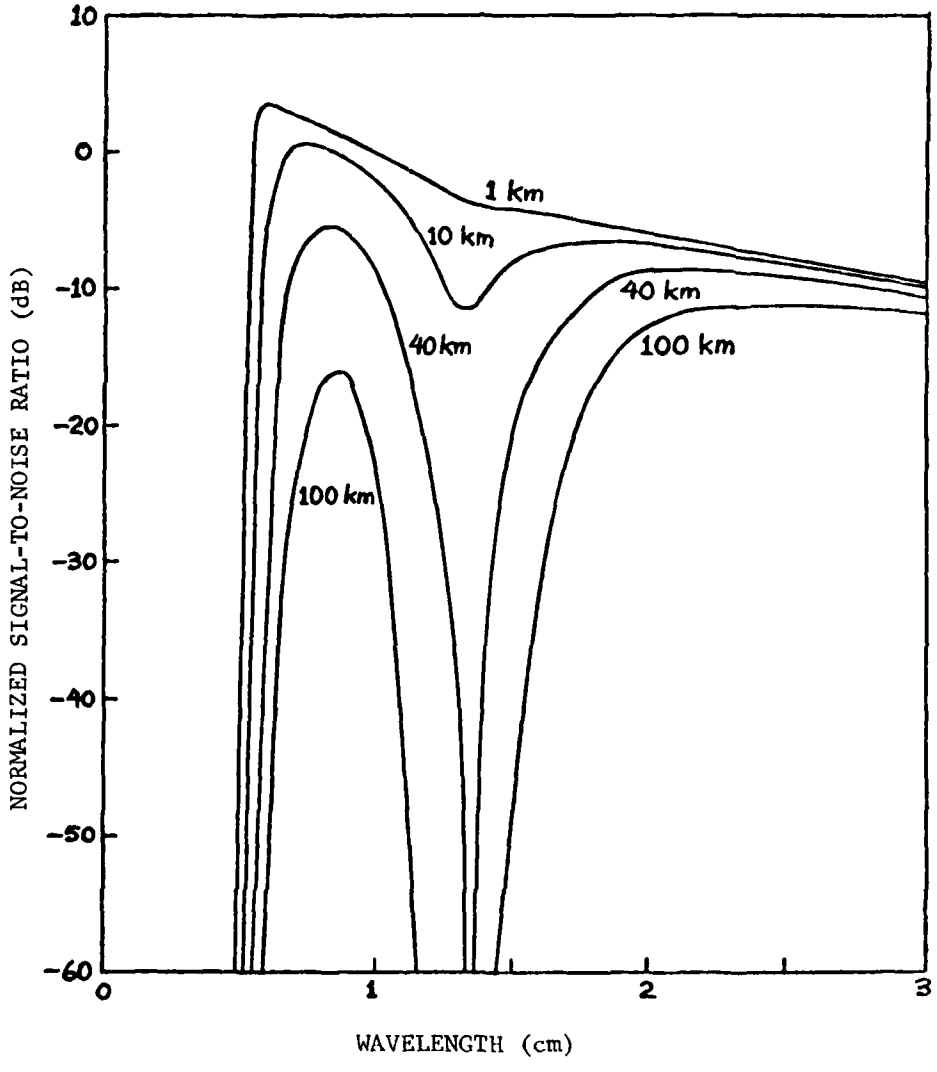

Figure 13. Normalized signal-to-noise ratio for observation of meteorological targets through humid clear air.

Using these values and interpolating between them, graphs of $\gamma(\lambda)$ versus λ are shown in Figure 14 for various rain rates.

For a moderate rain rate of 12.5 mm hr^{-1} (1/2 in hr^{-1}), graphs of SNR/K(dB) versus λ for a rain-filled medium are shown in Figure 15 for various ranges. Again, the peaks in the SNR/K vs. λ curves occur at values of λ that depend on range. The values of λ at which these peaks occur are given in Table 3.

The optimum operating frequency for transmitting through a rain-filled medium is anywhere from S-band to K_a-band depending on target range. The optimum transmitting frequency band for target ranges up to 40 km is apparently, from Figure 15, 4 GHz to 6 GHz. In this band of frequencies, SNR/K does not fall below -20 dB for target ranges up to 40 km. Lower frequencies are optimal for targets at longer ranges. Therefore, the optimal transmitting frequency for detecting hydrometeor targets in a moderate rainfall propagation medium is in S-band or C-band.

TABLE 3. WAVELENGTH AND FREQUENCY FOR WHICH NORMALIZED SIGNAL-TO-NOISE RATIO IS MAXIMUM (PROPAGATION THROUGH MODERATE RAIN)

r(km)	SNR/K Maximum
1	0.85 cm (35 GHz)
10	3.3 cm (9 GHz)
20	6.0 cm (5 GHz)
40	7.1 cm (4.2 GHz)
100	9.1 cm (3.3 GHz)

Graphs of SNR/K versus λ for targets at the maximum range in the primary region of coverage (40 km) are shown in Figure 16 for various rainfall rates. A transmitting frequency in X-band, K_u-band, or even K_a-band would be adequate for detecting meteorological targets in a light rain propagation medium.

The optimum transmitting frequency bands for detection of meteorological targets for various target ranges and propagation

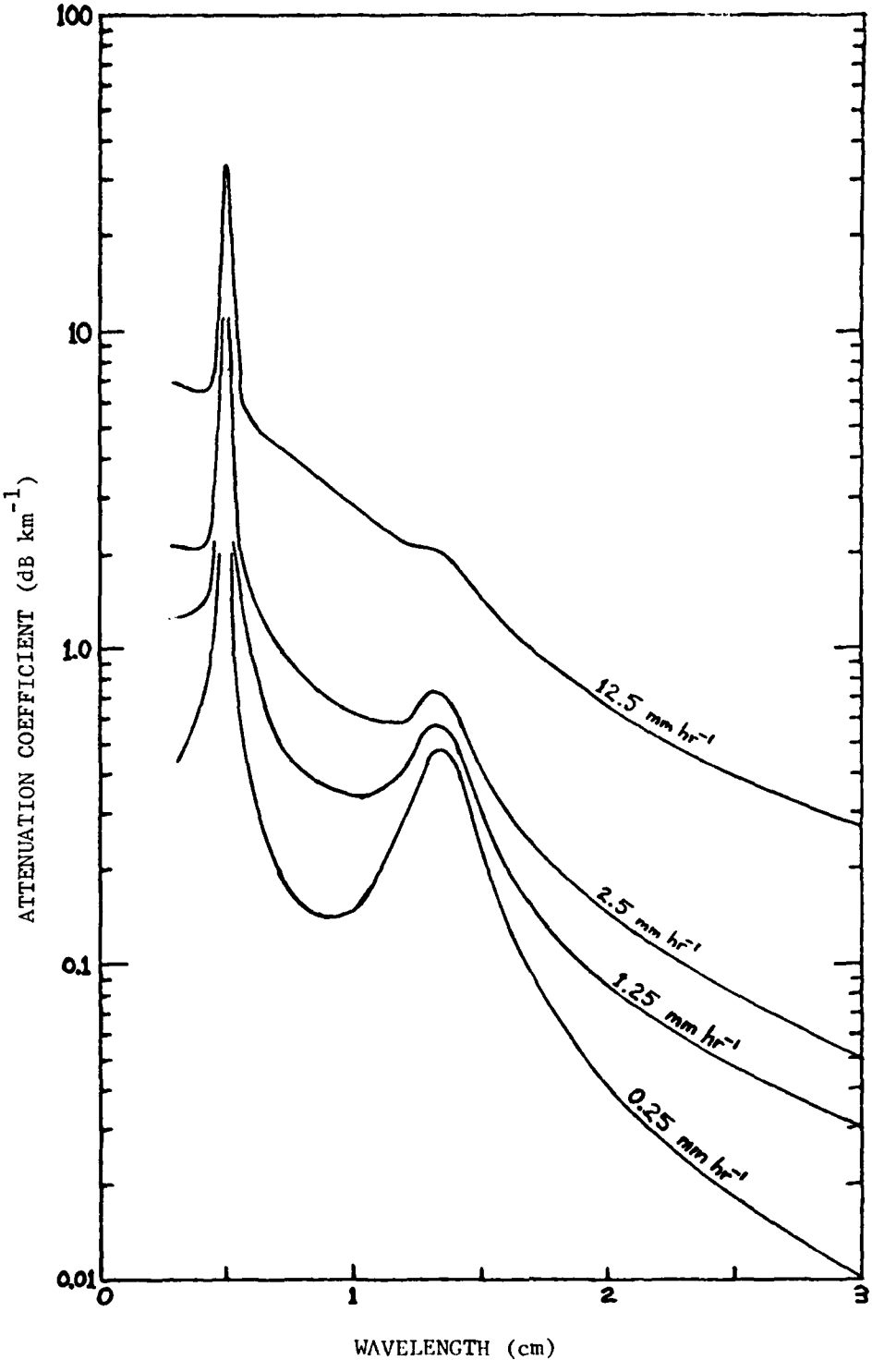

Figure 14. Attenuation coefficient due to absorption by atmospheric gases and rain.

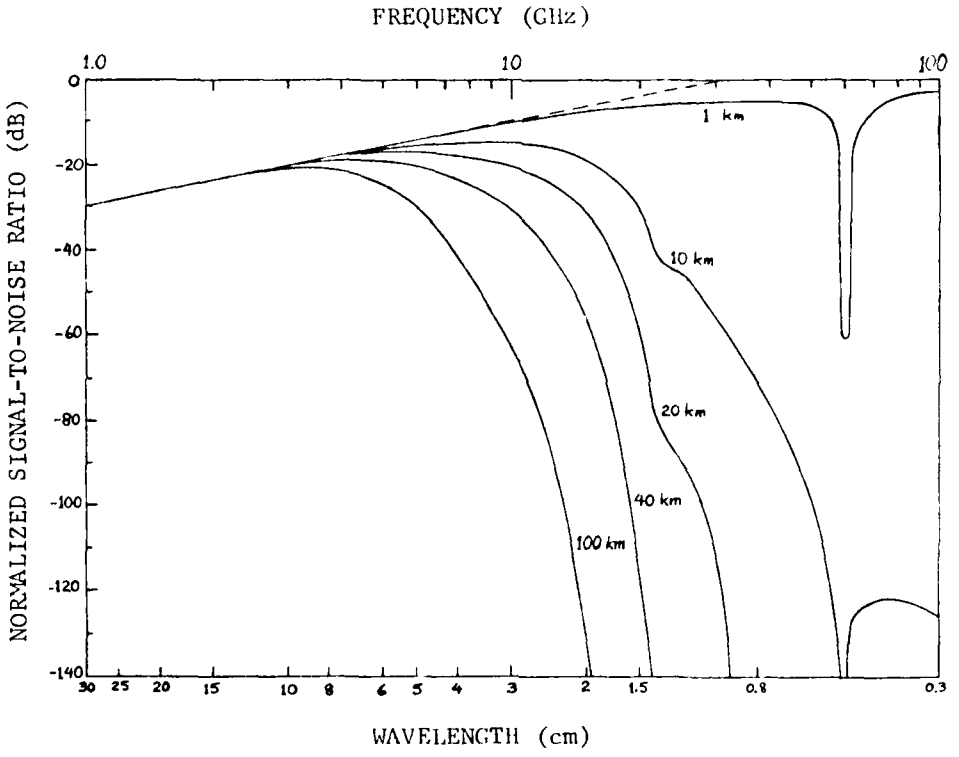

Figure 15. Normalized signal-to-noise ratio for observation of meteorological targets through moderate rain (12.5 mm hr^{-1}).

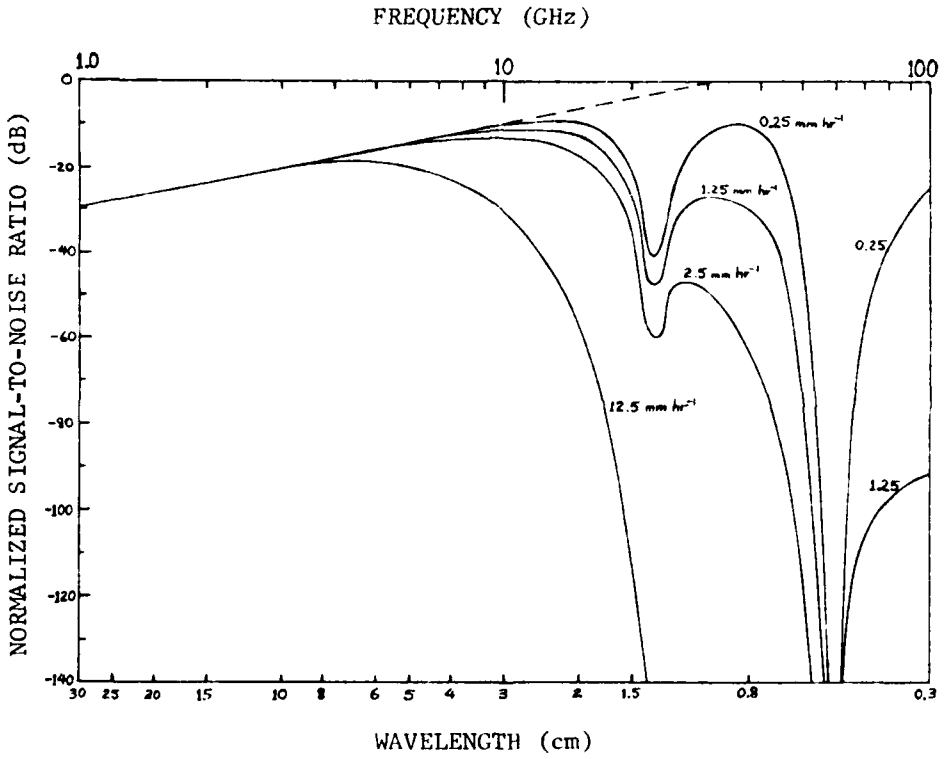

Figure 16. Normalized signal-to-noise ratio for observation of meteorological targets through rain at a distance of 40 km.

scenarios are summarized in Table 4. The choice of one transmitting frequency for all measurement scenarios is obviously an exercise in compromise. The adequacy of a chosen frequency can be evaluated by determining whether an adequate SNR for detection can be obtained for each target (rain, snow, hail, clouds) at that frequency. Radar parameters such as pulse length, beamwidth, and peak power must be specified before calculating the SNR for a given measurement scenario. Therefore, the ranges of acceptable pulse widths and beamwidths and an adequate SNR for detection will now be specified. Then for a chosen radar frequency and measurement scenario, the peak power required for detection of each target will be determined as a function of acceptable pulse widths and beamwidths. If the peak power thus determined is within an acceptable (attainable) range, then the chosen frequency will be adequate.

TABLE 4. OPTIMUM TRANSMITTING FREQUENCY BANDS FOR METEOROLOGICAL TARGET DETECTION

	PROPAGATION SCENARIO		
Target Ranges	Clear Air	Light Rainfall	Moderate Rainfall
Near (0-2 km)	Low mm, K_a	K_a	K_a
Primary Coverage Region (0-40 km)	Low mm, K_a	K_a, K_u, X	C
Far (40-100 km)	K_a, K_u, X	X	C, S

Since the SNR increases as the square of the pulse width, a wide pulse would be desirable to enhance detection probability. Also, a wide pulse is desirable for coherent radars, since generally coherence is lost during pulse rise and fall times. Thus, the relative amount of time that coherence is maintained within a pulse increases with pulse width, and coherent Doppler

processing capability is enhanced. Range resolution, $c\tau/2$, is a factor that drives the pulse width down. However, this is not generally a problem in weather radars since the along-range dimension of meteorological targets tend to be large compared to $c\tau/2$. Therefore, a pulse width in the range of 0.5 to 2 microseconds seems reasonable.

Since the SNR increases with decreasing antenna beamwidth, a small beamwidth would be desirable to enhance detection probability. However, a lower bound on beamwidth is required to keep antenna size reasonable, since beamwidth is inversely proportional to the antenna's diameter. For example, a 0.5-degree beamwidth at X-band requires a 14-foot antenna. Assuming a pencil beam such that $\theta_{el} = \theta_{az}$, a beamwidth in the range of 0.5 to 2 degrees (8.7 to 35 mrad) seems reasonable. A single pulse SNR of 10 dB is adequate for detection.

A rain-filled propagation medium ($R = 12.5$ mm hr^{-1}) with the target at the maximum range (40 km) of the primary coverage region was chosen for the measurement scenario. A light precipitation rate of 5 mm hr^{-1} is chosen for the precipitation targets (rain, snow, hail), and a water content of 1 gm m^{-3} was chosen for the cloud targets.

An S-band frequency of 3 GHz and an X-band frequency of 10 GHz were chosen for the transmitting frequencies. Thus, from Figure 15, SNR/K = -20 dB for 3 GHz and SNR/K = -31 dB for 10 GHz for the above measurement scenario. A receiver noise figure of 5 dB and a system loss of 7 dB were chosen.

Using these parameters, we obtained the graph of P_t versus θ^2/τ^2 shown in Figure 17 for the different targets. In the ranges of acceptable pulse widths and beamwidths, the peak power required for detection of the precipitation targets varies from a low of 11.5 W to a high of 117 kW. Transmitters at S- to X-band with peak powers in this range are readily available. However, the peak power required for the detection of clouds varies from 2.57 MW to 39.3 GW. Clearly then, a transmitting frequency in the S- to X-band is not adequate for the detection

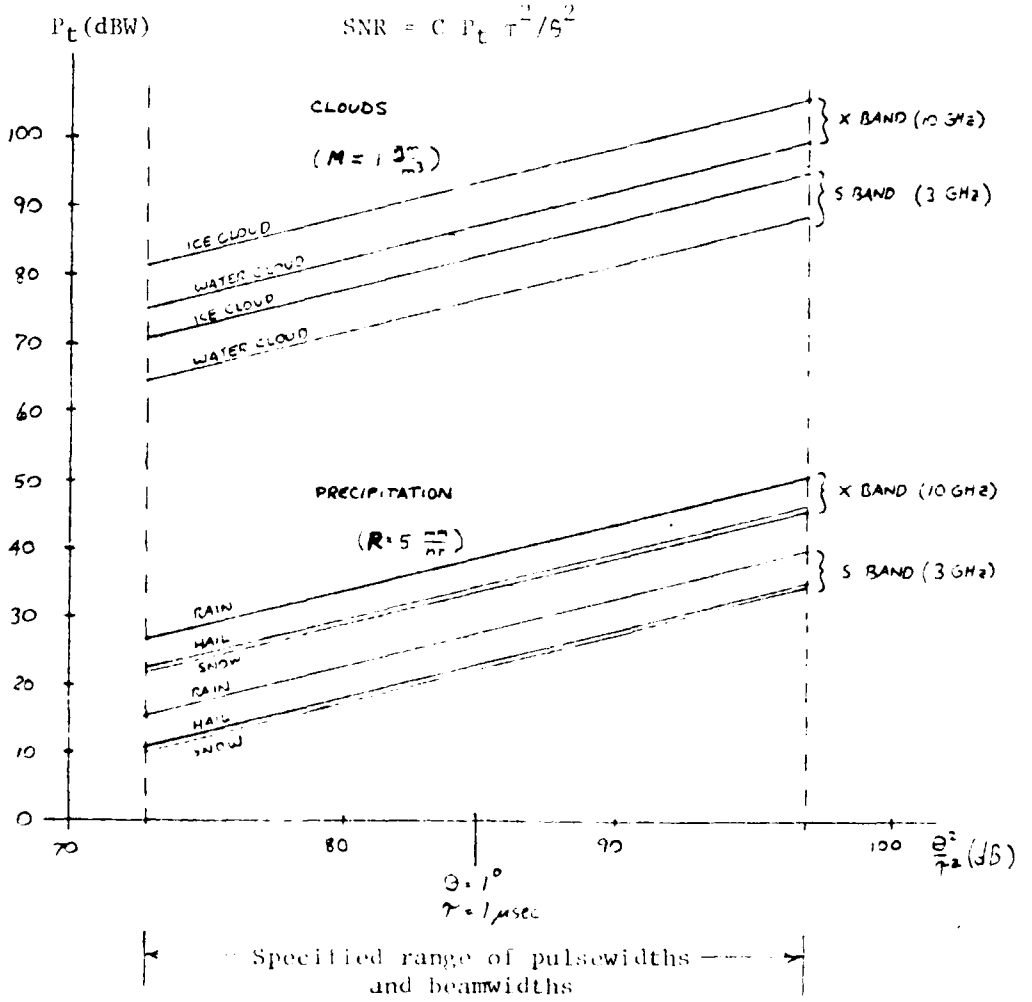

Figure 17. Required peak transmitted power P_t to achieve a 10-dB signal-to-noise ratio for observation of specified targets through moderate (12.5 mm hr^{-1}) rain at a range of 40 km, for a range of beamwidths and pulsewidths.

of clouds in the above measurement scenario. A 15 to 30 dB reduction in the required peak power is needed to bring it down to a realistic range attainable by radar transmitters. This reduction would have to be balanced by a corresponding increase of 15 to 30 dB elsewhere in the radar equation to maintain a 10 dB SNR. Instead of a SNR/K = -20 dB, SNR/K must now be no smaller than -5 dB for the same measurement scenario. Cloud detection thus requires a different measurement scenario, i.e., shorter target range, and a clear air or light rainfall propagation medium. For example, water cloud detection is possible with a radar transmitting frequency in X-, K_u-, or K_a-band and a peak power of 100 kW for cloud ranges of 10 km or less in a propagation medium with rainfall of 2.5 mm hr^{-1} or less. Optimal cloud detection occurs in clear air, short target range scenarios with a radar transmitting frequency in K_a-band.

Cloud detection at lower radar transmitting frequencies is also possible at shorter target ranges with the high power transmitters currently available at those frequencies. For example, with an operating frequency of 3 GHz and a peak power of 1 MW, the maximum cloud detection range is approximately 6 km for a one microsecond pulse width and a one-degree beamwidth.

In conclusion, while no one transmitting frequency is optimum for detecting all meteorological targets in all measurement scenarios, a transmitting frequency in the S- to X-band range is adequate for detecting all precipitation targets for all propagation scenarios and all the target ranges depicted in Table 4. (X-band frequencies may prove inadequate for very long-range targets in the moderate rainfall propagation scenario.) Cloud detection is possible at short target ranges in clear air or light rainfall propagation media and with high (K_a-band) transmitting frequencies. In addition to cloud detection, a frequency in K_a-band is optimal or adequate for precipitation target detection in some other measurement scenarios, such as clear air/light rainfall in the primary coverage region and moderate rainfall at short ranges. Cloud detection is also possible at low (S-band)

transmitting frequencies at short range with high transmitted power.

C. POLARIZATION

The measurement of hydrometeor shape and orientation parameters requires the reception of signals with polarization identical and opposite to that of the transmitted signal. The preceding subsection dealt with the detection of the "main" signal (i.e., the parallel-polarized linear component or the opposite-sense circular component). Because the power in the "orthogonal" signal (i.e., the cross-polarized linear component or the same-sense circular component) is typically 10 to 30 dB or more below that of the main signal, the sensitivity of the radar must be increased accordingly over that required for marginal detection of the main signal. Achieving the required system sensitivity is not generally difficult. The measurement of the orthogonal signal appears to be limited primarily by the isolation between the two channels at the antenna. The accurate interpretation of the orthogonal signal and of its cross-correlation with the main signal depends on the extent to which it is contaminated due to lack of channel isolation and due to depolarizing effects in the propagation medium.

A meteorological research radar with polarization diversity should be capable of transmitting and receiving right and left circular polarizations and linear polarization of arbitrary orientation to maximize polarization measurement capability. For example, a radar with both linear and circular polarization diversity provides the maximum versatility in raindrop canting angle measurements, in that at least three methods are available for the measurement. In the first method, circular polarization is transmitted and canting angle is determined from the phase of the cross-correlation of the two received signals. In the second method, canting angle is determined by transmitting linear polarization and rotating the plane of polarization until the depolarization is minimized. Finally, in the third method, if both linear and circular polarizations are transmitted sequentially,

then canting angle can be determined from the ratio of signals received in the linear and circular orthogonal channels. Elliptical polarization could be useful for a few purposes, such as evaluation of rain clutter cancellation techniques, but is not as important as circular and linear polarizations for the type of measurements we contemplate.

The main effect polarization has on the choice of an operating radar frequency is through depolarization of the signal in the propagation medium. Information about the meteorological targets in the resolution cell can be obtained through target-induced depolarization of the signal. However, if any signal depolarization occurs in the propagation medium, then target-induced depolarization effects are masked. If target depolarization characteristics are desired, then the transmitting frequency that maximizes the ratio of the target induced depolarization to propagation induced depolarization is appropriate.

Depolarization effects are negligible in a clear air propagation medium. Therefore, since target induced depolarization is nearly independent of operating frequency, at least in the Rayleigh scattering approximation, any radar transmitting frequency is acceptable as far as polarization is concerned. In a rain-filled propagation medium, depolarization increases with transmitting frequency and path length. Therefore, the lowest allowable transmitting frequency should be chosen to minimize propagation depolarization effects. This is demonstrated in Figure 2 of Section II. There, a measure of the ratio of propagation-induced depolarization to target-induced depolarization is given by the quantity $2p/v$. Propagation induced depolarization effects can be neglected when $2p/v \leq 0.1$. Therefore, from Figure 2, short target ranges and low radar transmitting frequencies are necessary to negate propagation depolarization effects when light rain is in the propagation medium. For example, for $R=2$ mm hr^{-1} and $r = 5$ km, the radar operating frequency must be 4 GHz or less for $2p/v \leq 0.1$.

Propagation depolarization effects through rain can be greatly reduced with the use of linear polarization. Theoretically, propagation depolarization effects can be virtually eliminated if the plane of polarization is aligned with one of the mean principal axes of the raindrops; i.e., the polarization vector is aligned with, or at right angles to, the mean canting angle of the raindrops in the propagation medium. However, if the target is this same collection of raindrops, then target-induced depolarization is also minimized and available information is lost. Linear polarization is effective in scenarios where the radar is observing hail or snow through rain. Both horizontal and vertical polarizations must be transmitted to gain the same amount of polarization information as is obtainable with a circularly polarized signal. These transmitted polarizations should be as close together in time as possible. Pulse-to-pulse polarization agility would be desirable.

In conclusion, while detection criteria of precipitation targets allow an operating frequency in the S- to X-band range, polarization considerations drive the choice of frequency to the lower end of that spectrum, i.e., to S-band. An S-band frequency is also adequate for cloud detection at short ranges with high power transmitters. Optimum cloud detection occurs at high transmitting frequencies (K_a-band), short ranges, and clear air: a measurement scenario yielding negligible propagation-induced depolarization.

D. MULTIPLE FREQUENCIES AND FREQUENCY MODULATION

In the development of a meteorological remote sensing system, the question arises as to whether the measurement capability would be enhanced by the joint use of sensors at more than one frequency, such as two radars or a radar and a lidar. Furthermore, since frequency modulation techniques have been used successfully for several meteorological applications it is essential to consider their possible utility in the context of a coherent dual-channel radar.

There are two facets of the multiple frequency question: first, whether the use of two (or more) transmitting frequencies provides any increase in the capability of measuring or deriving the parameters of interest at a given point, and second, whether it is desirable to operate two or more sensors of different characteristics at the same time to observe a wider range of hydrometeor types.

Multiple frequency radar observations have been used for the detection of hail, based on the frequency-dependent scattering and attenuation characteristics of hail and rain. The hail detection capability is based on Mie scattering characteristics of hail and on the greater attenuation encountered in both rain and hail at the higher microwave frequencies (C-band and X-band). To the extent that the Rayleigh scattering approximation is valid, the information obtained from the scattering medium is redundant, except that the attenuation encountered at the higher frequency (relative to the negligible attenuation at S-band) gives an additional estimator of the rainfall rate or water content in the propagation medium. Because the backscatter polarization characteristics of raindrops are nearly independent of radar frequency, the use of two frequencies would not improve this measurement capability. While a frequency in X-band, for example, would permit better detection of small raindrops and of snowflakes, such detection could also be accomplished at S-band if adequate power is used. In summary, we conclude that the use of two frequencies for observations of precipitation would not add significantly to the system measurement capability. It would, however, be useful to have a "head-to-head" comparison of dual-frequency hail detection and dual-channel hail detection to understand better the strengths and weaknesses of both techniques.

In the context of cloud observations, the possibility of observations by lidar must be considered, since lidar has been proven capable of discriminating ice and liquid water clouds and of identifying shapes of ice particles in some situations.[3] The

relative capabilities of lidar and radar for the detection of clouds were investigated by Derr.[15] He found that for detection of the near edge of several model clouds a CO_2 (10μm) lidar was superior to various radars in all cases, except when rain was present. The lidar superiority over a short-wavelength radar was no greater than about 7 dB in any of the cases. In the scenario of 1,000 m penetration into a cloud at a distance of 5,000 m to the near edge, the results were mixed. Derr suggested that joint observations with radar and lidar were desirable for investigating the development of clouds and the onset of precipitation within them.

For measurement of the shape and orientation of cloud water drops or ice crystals, we must consider not only detection criteria but also the relative capabailities for obtaining polarization-related information. Lidar measurements typically have included the depolarization ratio and, in some cases, the signal intensity or reflectivity. The pulse characteristics of lidars permit the interrogation of a given array of hydrometeors only once and thus do not allow the derivation of the signal cross-correlation. The average orientation angle of the scatterers would be derivable by successive observations at varying polarizations. Radars operating at pulse repetition frequencies of several hundred hertz or more obtain a series of observations of a given array of hydrometeors, i.e., before the scatterers move through the resolution cell. From the time series, one can obtain the power spectra and cross-spectrum in addition to the average power, depolarization ratio, and cross-correlation. Thus, the advantages of lidar lie mainly in extending the measurement capability to clouds of low water content and small crystals or drops, rather than in enhancing the measurement capability in the situations where target detection by radar is adequate.

Multiple frequencies have also been used to resolve ambiguities of Doppler velocity measurements resulting from spectrum folding. Since we contemplate the use of a low frequency for

[15] Derr, V.E., 1978: A Basic Comparison of Lidar and Radar for Remote Sensing of Clouds. Technical Report ERL 397-WPL 52, Nat'l. Oceanic and Atmospheric Admin.

observations at low elevation angles and long ranges, we do not anticipate that spectrum folding will be a problem in most situations. At higher elevation angles, higher PRFs can be used to increase the limits of unambiguous Doppler velocity. The need for unambiguous measurement of Doppler velocities above 20 m sec^{-1} in severe storms while preserving unambiguous range information can be met by means of a radar which transmits at two frequencies in a single microwave band. One frequency is pulsed slowly enough that reflectivity measurements can be obtained with no range ambiguity, while the other is pulsed fast enough that Doppler velocities are measured unambiguously, with possible range aliasing. This technique could be incorporated into a dual-polarization radar design, with either or both frequency channels doubled for reception of two polarizations. In principle, it would be desirable to have dual-polarization reception on both frequencies, since in a situation in which two storms were separated in range by a distance equal to the maximum unambiguous range in the Doppler channels, the Doppler velocity information would be unusable, while the "bulk" polarization parameters could still be obtained in the reflectivity channels. The feasibility of implementing such a design depends on the frequency dependence of components of the microwave circuit and antenna. In practice, the use of both circular and linear polarization requires dual polarization on the "reflectivity" frequency since the reflectivity information would be obtainable in the opposite polarization and the identical polarization, respectively, for the two transmission modes. Since most of the polarization information available in the reflectivity channels would be completely redundant with that available in the Doppler channels for most measurement scenarios, dual-polarization reception and full data processing need be implemented only for the frequency to be used for Doppler measurements, and the range information in the reflectivity channel can be used to de-alias the polarization information as it is used to de-alias the Doppler velocity information.

The use of frequency modulation techniques is of interest because they enable more rapid determination of average signal characteristics by reducing the "phase noise" in the received signals associated with the random relative motion of the scatterers in phase space. In the context of dual polarization radar observations, one must consider the frequency-dependence of the polarization characteristics of radar components and the extent to which performance may be degraded if the transmitted signal bandwidth is increased. As an example, in the 16.5 GHz radar operated by the National Research Council (NRC) in Ottawa, Ontario,[16] the frequency stability requirement is determined by the bandwidth of the turnstile junction in the antenna feed, which is about 0.1 per cent of the center frequency, or $\pm$ 8 MHz. Hence, the NRC antenna design is incompatible with the use of wideband techniques such as that used by Krehbiel and Brook.[17] Alternative antenna designs, discussed in Section V, will permit the use of wideband transmission. The use of wideband or frequency-modulated transmission and the achievement of the associated fast-scanning capability will be necessary for the effective study of certain physical phenomena. For example, the changes of hydrometeor polarization properties which accompany electrical discharges have been well documented[18] at time scales of the order of one second at fixed antenna position. Reflectivity changes associated with electrical discharges have been measured by Brook (private communication) at time scales of the order of a few milliseconds. Hence, it is evident that the complete documentation of electrical effects in both space and time

16 McCormick, G. C., and Hendry, A., 1979: Techniques for the Determination of the Polarization Properties of Precipitation. Radio Sci., 14, 1027-1040.

17 Krehbiel, P. R., and Brook, M., 1979: A Broad-Band Noise Technique for Fast-Scanning Radar Observations of Clouds and Clutter Targets. IEEE Trans. Geosci. Electr., GE-17, 196-204.

18 McCormick, G. C., and Hendry, A., 1979: Radar Measurement of Precipitation-Related Depolarization in Thunderstorms. IEEE Trans. Geosci. Electr., GE-17, 142-150.

will require a rapid scanning capability. The incorporation of measured Doppler velocity data into computer models of severe storms requires observations at much shorter time scales than are presently available and hence requires that fast-scanning capability be available in a future generation of meteorological Doppler radars. It will eventually be necessary to incorporate polarization-related parameters into computer models for verification and updating of cloud and precipitation physical parameters; this will require that the polarization parameters be available with high temporal resolution.

The implementation of fast-scanning capability into a dual-polarization polarization-agile system requires detailed evaluation of the performance of the microwave components in terms of bandwidth, phase stability, and dispersive (frequency-dependent) characteristics, which are beyond the scope of the present study. The effective use of the data obtainable from a fast-scanning radar requires either a much higher capacity data-processing system or that much of the data processing be done off-line. While a fast-scanning radar would provide measurements of reflectivity, Doppler mean velocity and variance, and bulk polarization parameters within acceptable statistical confidence limits, it is not evident that the spectral functions which are a key part of the interpretation of the dual-polarization backscatter can be computed with acceptable accuracy from fast-scanning radar data. Hence we recommend that the dual-polarization capability be implemented initially in a narrow-band system, and that the analytical and interpretive techniques already suggested be further developed and refined on the basis of real data before proceeding to the development of a fast-scanning coherent dual-channel radar.

In summary, we conclude that the coherent polarization-diversity radar should be a single-frequency narrow-band system. For observations of rain, the use of a multi-band system adds little to the measurement of polarization parameters in a given scattering medium. The use of more than one frequency band does extend the range of measurement capability in terms of detectable

scattering media, but such observations tend to imply the use of multiple measurement systems, rather than the incorporation of the total capability into a single system. The limited polarization capabilities of lidar relative to those of radar similarly imply that the polarization properties of radar-detectable clouds can be adequately measured by radar alone. The use of frequency-modulation or wideband transmission for reducing backscatter "phase noise" and achieving a faster scanning capability is desirable, but likely to be difficult to implement in a coherent dual-channel radar system. The possibility of using wideband microwave components to accommodate such techniques is an important topic for further investigation.

E. SUMMARY

On the basis of the foregoing analysis, we conclude that the transmitting frequency options are S-band and K_a-band for measurements in precipitation and in clouds, respectively. The use of frequencies above S-band results in increasing propagation effects which degrade the backscatter measurement capability in moderate or heavier rain. Conversely, the use of frequencies lower than K_a-band results in rapidly decreasing sensitivity to backscatter from small hydrometeors. A matrix of measurement scenarios is given in Table 5, and the adequacy of the two frequency bands, S and K_a, for the particular scenarios is shown. A frequency band appears for a given scenario if it is adequate for most of the precipitation rates (or water contents) and target ranges for that scenario. In the cases where both frequency bands are shown, the one appearing first is preferred. If measurements only through a clear propagation medium are contemplated, then K_a-band is the preferred frequency band for all target types and ranges. However, measurements through a rain-filled medium will require a frequency in S-band and a consequent reduction of cloud measurement capability.

The polarization mode preferred for most measurements is circular, because of the resultant capability of determining the orientation state of the scatterers. For a broader range of

TABLE 5

COMPARISON OF K_a-BAND AND C-BAND OBSERVATIONS OF CLOUDS AND PRECIPITATION IN VARIOUS RADAR TARGETS IN SEVERAL PROPAGATION MEDIA

Target and Measurement		Propagation Medium							
		Clear Air			Light Rain (2.5 mm/hr)			Moderate Rain (12.5 mm/hr)	
		0-6 km	0-40 km	40-100 km	0-6 km	0-40 km	40-100 km	0-6 km	0-100 km
No Polarization Measurements	Precipitation Targets	K_a,S	K_a,S	K_a,S	K_a,S	S,K_a	S	K_a,S	S
	Cloud Targets	K_a,S	K_a	-	K_a,S	-	-	K_a,S	-
Polarization Measurements	Precipitation Targets	K_a,S	K_a,S	K_a,S	S,K_a	S	S	S	-
	Cloud Targets	K_a, S	K_a	-	S, K_a	-	-	-	S

possible measurement objectives, it is desirable to have available both circular and linear polarizations with variable orientation.

Other desirable radar parameters include a pulse width of 0.5 to 2 μsec a beamwidth of 0.5 to 2 degrees, a pulse repetition frequency variable from about 300 Hz to 10 kHz, and a peak power of at least 100 kW. Full scanning capability in azimuth and elevation is, of course, essential for the measurement objectives.

The implementation of these design parameters is expected to be essentially similar at the two proposed frequencies. A description of the suggested microwave system is presented in Section IV and antenna design factors are discussed in Section V. The data system described in Section VI can be used with either radar, since operation at either of the two recommended frequencies will involve measurements at relatively high elevation angles and high pulse repetition frequencies. It is in this mode of operation that the data rates are highest. Operation at low elevation angles for long range measurements, which will not be possible at K_a-band, involves lower pulse repetition frequencies because of the need for large unambiguous range limits.

SECTION IV
SYSTEM CONFIGURATION

The general concepts discussed in this section are equally applicable to a radar system operating at either of the two frequency bands identified in the preceding section. In accordance with the decision based on preliminary results of this study, we have given detailed consideration to component limitations and availability only for a radar system operating at S-band (10 cm wavelength). The objective of this effort is to present a design for a radar system which permits the collection of appropriate radar signals to quantify a variety of hydrometeor microphysical parameters. The types of hydrometeors and associated parameters have been described in detail in Section II. To obtain the greatest possible information from the hydrometeor backscatter signal, the radar system should be coherent, dual polarized, and polarization agile. The design implications of these characteristics will be discussed in this section with respect to system requirements imposed by the hydrometeor targets.

Before proceeding further, clarification of terminology is in order. Imposition of coherence on the radar system means that the baseband radar video signal at the output of the radar contains both amplitude and phase information. The phase information of this signal is relative to the phase of the transmitted pulse, while the amplitude information is simply the magnitude of the return. Coherence of the transmitted signal from one pulse to another will depend on the actual implementation of the transmitter module and is necessitated only when concerned with returns from targets at ambiguous ranges, i.e., ranges beyond the maximum ambiguous range determined by the system pulse repetition rate.

Dual polarization is defined as the capability of simultaneously receiving the same polarization as was transmitted plus the oppositely polarized return. In the conventional radar terminology, especially with reference to linear polarization, these

signals are referred to as the "parallel" or "co-polar" and the "cross" components of the backscattered signal. The term "orthogonal" is also used to describe the oppositely polarized signal, but this nomenclature is a source of confusion in radar meteorology because the term "orthogonal" has also been used to refer to that circular polarization component of the return from rain which is opposite to the "main" signal that contains the larger portion of the backscattered power. We shall use the terms "parallel polarized" or "co-polar" to refer to the received signal in the transmission channel and "cross-polarized" to refer to the received signal in the orthogonally polarized channel, regardless of the polarization state of the transmitted signal.

Polarization agility is the capability of rapidly changing the polarization state of the transmitted pulse, that is, at least as fast as the pulse repetition rate. The term polarization diversity refers only to the ability to change the transmitted polarization, with no rate of change implied. Thus dual polarization (on receive) and polarization agility (on transmit) are different system attributes, although either capability impacts the implementation of the other.

Within the definition above, a radar system providing polarization diversity will meet some of the present requirements. However, time decorrelation of the meteorological target occurs much more rapidly than the switching period associated with polarization diversity and adversely affects the relationship of the parameters being measured. A polarization-agile system will allow measurement of the parameters for two transmitted polarizations, spaced in time by the interpulse period. In addition, the polarization agile system which is described will allow an unlimited selection of polarization modes, depending on the type of antenna feed selected and the parameters to be controlled.

A. GENERAL CONCEPTS

The polarization of an electromagnetic wave can be described by specifying the amplitude and electrical phase between two spatially orthogonal phasors. Circular polarization can be

generated by combining two orthogonal linearly polarized signals; conversely, linear polarization can be generated by combining two orthogonal circularly polarized signals. In the most general sense, two orthogonally polarized signals will produce an elliptically polarized wave with the limiting cases being circular and linear polarizations. These principles are employed in the radar shown in Figure 18 to implement a polarization-agile system. In this system, the polarization of the transmitted and received signals are determined by the phase and amplitude of the signals present at the two orthogonal ports of the dual mode coupler and by the antenna feed system. The signal at the output of the dual mode coupler is described by

$$E_T = iE_1 \sin \omega t + j E_2 \sin(\omega t + \theta) \qquad (23)$$

where i and j represent the space vectors, and $E_1 \sin \omega t$ and $E_2 \sin(\omega t + \theta)$ represent the amplitude and phase of the two input signals. Equation (23) in general defines an elliptically polarized wave which can be described in terms of the relative phase θ and the ratio $E_1/E_2 = \alpha$. The phase and amplitude ratios of the input signals to the dual mode coupler required to generate linear and circular polarization for a linear antenna feed system are shown in Table 6. For other values of θ and α, the transmitted signal will be elliptically polarized. The axis of the polarization ellipse and the ellipticity ratio will depend on both θ and α. If the two signals are in phase or 180° out of phase, the resulting polarization will be linear; the plane of polarization will be determined by the relative amplitudes of the two signals.

If a circular polarizer is placed at the output of the dual mode coupler, a different set of polarization control parameters are required as shown in Table 7. For this case, orthogonal circular components are combined to produce a system capable of transmitting and receiving any desired linearly or elliptically polarized wave. The phase angle (θ) between the two orthogonal ports of the dual mode coupler controls the axis of either the

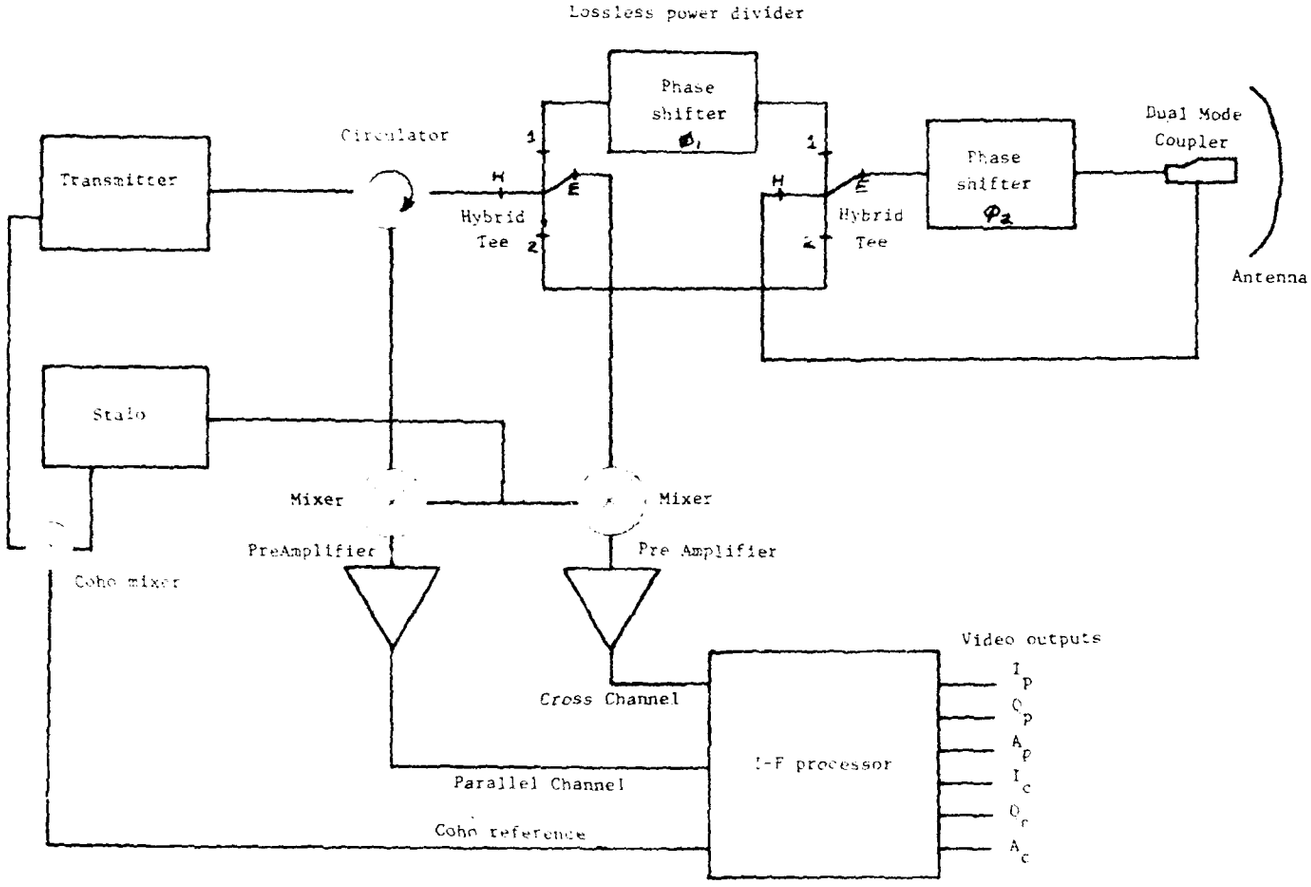

Figure 18. Polarization diversity radar.

elliptical or the linear signal, and α controls the ellipticity ratio.

TABLE 6. TRANSMITTED POLARIZATION AS A FUNCTION OF θ AND α FOR A LINEARLY POLARIZED FEED

Polarization	θ (degrees)	α
Linear 45°	0	1
Linear -45°	180	1
Circular RH	90	1
Circular LH	-90	1
Vertical	any value	0
Horizontal	any value	∞

TABLE 7. TRANSMITTED POLARIZATION AS A FUNCTION OF θ AND α FOR A CIRCULARLY POLARIZED FEED

Polarization	θ (degrees)	α
Linear	any value	1
Circular RH	90	0
Circular LH	-90	∞
Elliptical	any value	$0<\alpha<1$

Thus, controlling the phase and amplitude of the signals at the input of the dual mode coupler allows a very versatile selection of polarizations.

Polarization control of the radar shown in Figure 18 is accomplished by changing the phase of the signals in the lossless power divider and by changing the phase of one of the signals to the dual mode coupler. The lossless power divider is composed of two hybrid tees and an electronically controlled phase shifter.

The first hybrid tee divides the input power equally between its two collinear output ports. One of the outputs is shifted in phase and recombined in the collinear arms of the second hybrid tee. The ratio of power available at the E and H ports of the second hybrid is determined by the phase difference between the signals supplied to the two input ports according to

$$\frac{P_E}{P_H} = \tan^2 (\phi/2) = \alpha \tag{24}$$

For the circularly polarized antenna feed, the phase angle ϕ_1 in the power divider controls the ellipticity of the transmitted wave, and the phase angle ϕ_2 controls the axis of the resultant elliptical or linear signal. In the case where a linearly polarized antenna feed is employed, both ϕ_1 and ϕ_2 contribute to the ellipticity of the resultant signal.

The two hybrid junctions in the lossless power divider influence the purity of the transmitted wave and the channel isolation of the receiver. For near-spherical raindrops, one component of the reflected signal will in many cases be more than 20 dB below the other. Since the ratio of the powers in the two orthogonal channels is one of the major parameters to be measured, polarization purity and channel isolation must be maintained to prevent large measurement errors. It is instructive for the purpose of describing the purity of the transmitted and received signals to determine the phase error present at the output ports of the hybrid tees. The phase angle of the two output signals from the E and H ports is given by

$$\phi = \tan^{-1} \frac{2\alpha \sin\theta}{1 - \alpha^2} \tag{25}$$

where α is the ratio of the voltages present at the two collinear input ports and ϕ is the phase difference between the two voltages. When ϕ is near 90 degrees, the phase angle is primarily determined by the power ratio α^2, at the input ports. Power balance and proper phasing of these signals must be maintained at the dual mode coupler to preserve measurement accuracy. For this

reason, it is important that some form of power monitoring be included in the radar system.

B. RADAR CONFIGURATION

A radar system using the concepts described above is shown in Figure 19. If pulse-to-pulse polarization agility is to be achieved, electronic phase shifters must be used to provide the high switching rates. The power handling capability of electronic phase shifters is limited to 100-200 kW peak for non-reciprocal devices and to 25 kW peak for reciprocal devices. Peak power of the order of 1 mW is necessary to achieve the desired measurement objectives. The polarization switching must therefore be accomplished at low power levels, and the resulting signals must be amplified to the required level. Because the microwave amplifiers in the system do not allow reciprocal propagation of the received signals, two identical polarization networks must be used. The first network is used to control the desired power balance and phase relationship between the two signals applied to the dual mode coupler. The second polarization network is used in the receiver to derive the parallel and cross polarized components of the backscattered signal.

Accurate phase and amplitude tracking characteristics must be maintained in both transmitter amplifier chains and between the phase shifters in the transmitter and receiver. A directional coupler (not shown) is included at the output of the circulators to provide for power monitoring and to allow a test signal to be injected into the receiver for calibration. Power balance sensing and automatic correction should also be included.

The transmitter shown as a block in Figure 19 contains the necessary oscillators, phase lock loops, and multipliers to generate the signal to be transmitted, the local oscillator signal, and the IF coherent phase reference for measurement of the in-phase (I) and quadrature (Q) components of the received signals.

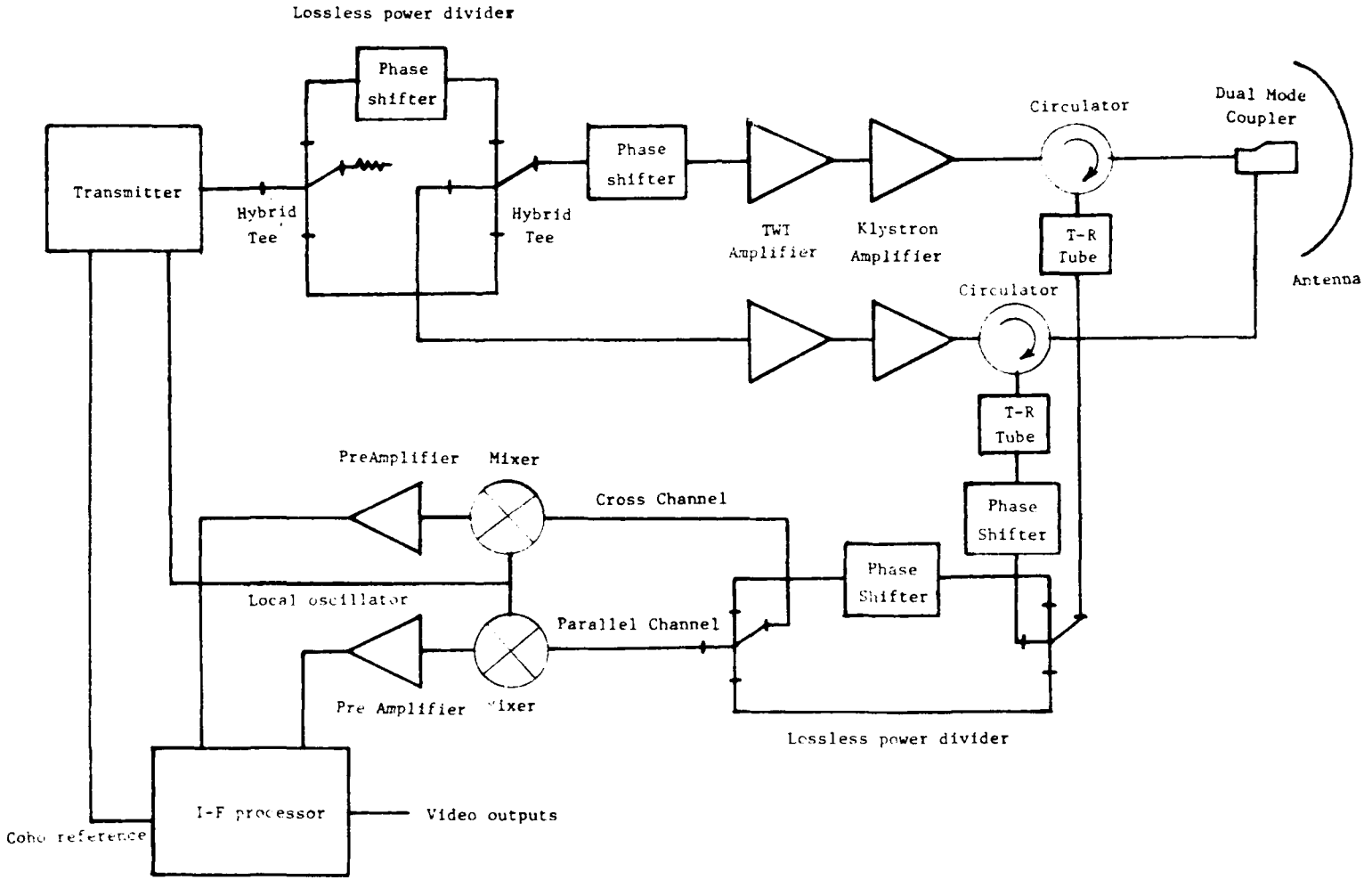

Figure 19. Polarization agile radar with polarization switching accomplished at low power level.

SECTION V
ANTENNA CONSIDERATIONS

A study was performed to determine some of the trade-offs involved in realizing the antenna portion of the coherent polarization diversity radar. This evaluation included (1) the RF plumbing required to obtain dual switchable polarization, (2) the method of switching, (3) the impact of utilizing different frequency bands, as well as (4) the type of antenna itself.

The types of polarization considered were dual circular and dual linear. The radar must be able to transmit using one polarization and be able to receive the same polarization that was transmitted, as well as the cross polarization. In addition, the radar should be able to transmit either of the two orthogonal polarizations. For example, the radar might transmit vertical polarization and receive both vertical and horizontal polarization. It might then switch to transmitting horizontal polarization and still receive both vertical and horizontal polarizations. Initially, because the frequency of operation had not been finalized, K_a, C, and S band operations were considered. The desired beamwidth of the antenna is about 1.0^{o}.

A. ANTENNA TYPES

This study was restricted to considering only reflector type antennas since a mechanically scanned, narrow beam antenna is adequate for the intended application. The flexibility of an electronically scanned array is not needed and the price of this option is very high. The antennas of primary interest for this application are parabolic and Cassegrain reflectors in either center fed or offset fed geometries.

1. PARABOLOIDS

The paraboloid is the most commonly used reflector type because it will produce a high-gain pencil-beam with quite low sidelobes when properly fed from the focal point. The parabolic

antenna had its birth in 1888 with the experiments of Heinrich Hertz, and the properties of parabolic antennas have been extensively studied both theoretically and experimentally since World War II. The following discussion is oriented toward polarization characteristics of the antennas since this is the major area of uncertainty in the performance of the antenna system under study.

Jones[19] studied the polarization properties of a circularly symmetric paraboloid that is fed by a short electric dipole at its focus. He found that the cross-polarized pattern of such antenna systems consists of four major lobes symmetrically located along the 45^{o} planes (i.e., between the principal planes). Figure 20 shows the level of these lobes as calculated by Jones, neglecting aperture blockage produced by the feed. Also presented in Figure 20 are recent calculations by Bodnar[20] for the case of a paraboloid focus fed by a pyramidal horn, again neglecting blockage. The pyramidal horn is much more commonly used at microwave and millimeter wavelengths than is an electric dipole, and so it more nearly represents the cross-polarized performance expected from the antenna under study. The -10 dB and -20 dB pyramidal horns represents cases where the aperture size of the horn has been selected so that the horn illumination taper plus the space loss taper produces combined edge illuminations of -10 dB and -20 dB, respectively. Notice from Figure 20 that the level of the cross-polarized lobes decrease monotonically as the focal length of the reflector is increased and that a heavier edge taper produces lower cross-polarized levels. Also, lower cross-polarization is predicted for a pyramidal horn than for an electric dipole feed. For example; for a -20 dB pyramidal horn and a reflector having a focal length to diameter

[19] Jones, E. M. T., 1954: Paraboloid Reflector and Hyberboloid Lens Antennas, IRE Trans. Antennas Propag., AP-2, 119-127.

[20] Bodnar, D. G., 1980: Cross-Polarized Characteristics of Monopulse Difference Patterns, IEEE/AP-S Int'l. Symp., Quebec, Canada, June 2-6.

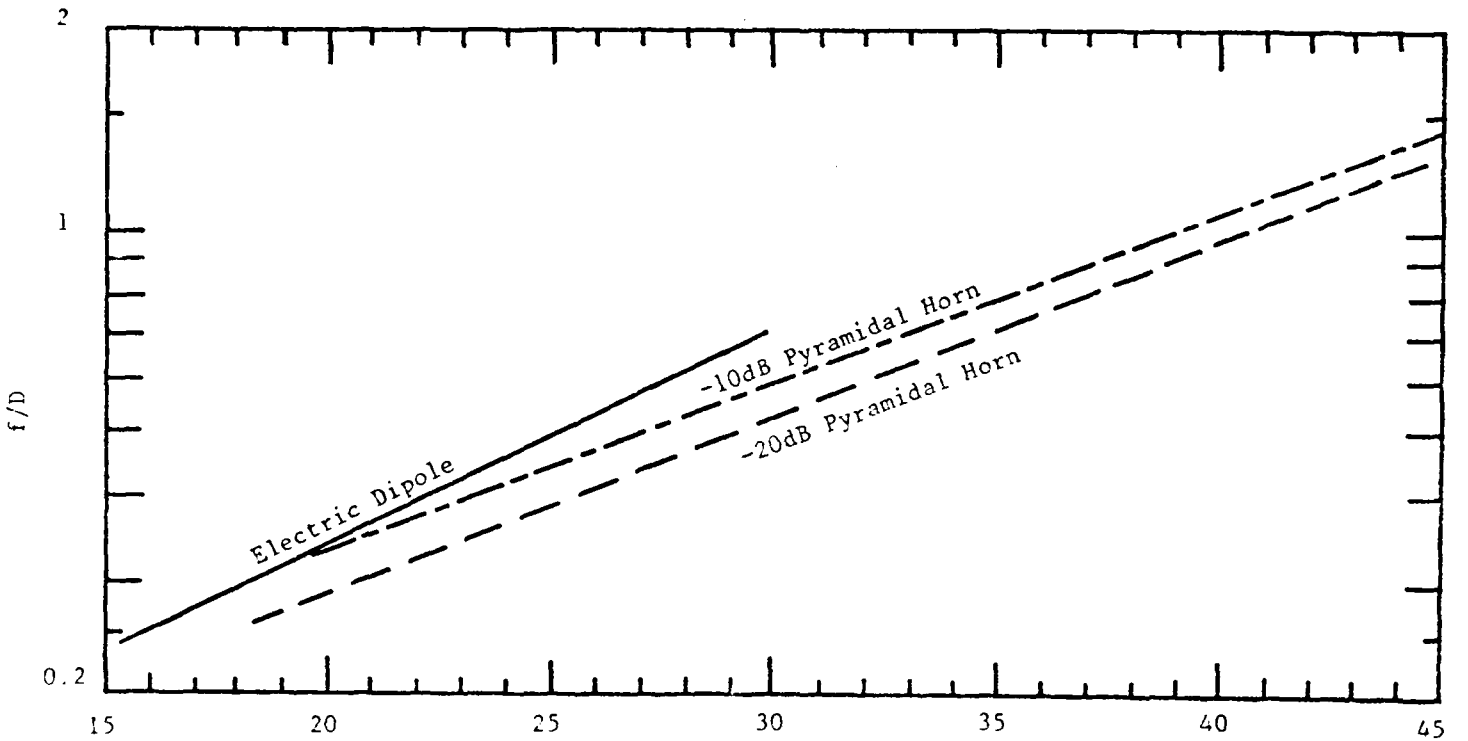

Figure 20. Peak cross-polarization level versus focal-length-to-diameter ratio for a symmetric, center-fed paraboloid.

ratio (f/D) of 0.25 or 1.0, the cross-polarized lobes are -18 dB and -40 dB, respectively, with respect to the co-polarized main beam peak.

Figure 20 shows that a long focal length reflector in conjunction with a highly tapered feed illumination is required to produce low cross-polarized lobes. The high feed taper also produces lower co-polarized sidelobes, which is usually desired. However, the use of a long focal length reflector and a high feed taper requires a large feed. A large feed, in turn, produces increased blockage of the energy reflected by the paraboloid which in turn increases the co- and cross-polarized sidelobes.

The effects of blockage can be reduced or eliminated by using an offset reflector geometry in which the feed is tilted to illuminate only a portion of the paraboloid that does not include the central area where the feed is located. Energy reflected by the paraboloid then does not strike the feed. Chu and Turrin[21] have analyzed the cross-polarized characteristics of offset fed paraboloids, and Figures 21, 22, and 23 present some of their results. Their feed is pointed at an angle of θ_o from the axis of the reflector, and θ_c is the half-angle subtended by the outer edge of the reflector at the focus.

Figure 21 shows that cross polarization is reduced by illuminating the paraboloid as close to its axis as possible. Figure 22 shows that when $\theta_o = \theta_c$ the cross-polarized characteristics are very similar to the -20 dB pyramidal horn curve of the center-fed paraboloid shown in Figure 20.

The preceding discussion is based on the use of a linearly-polarized feed. Figure 23 presents data for a circularly-polarized feed. For a circularly polarized feed, no cross-polarization is generated theoretically, but the right and left

[21] Chu, T. S. and Turrin, R. H., 1973: Depolarization Properties of Offset Reflector Antennas, *IEEE Trans. Antennas Propag.*, AP-21, 339-345.

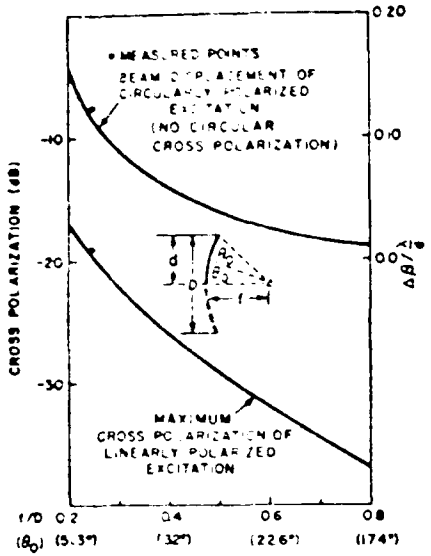

Figure 21. Cross polarization and beam displacement versus f/D ratio ($\theta_0=\theta_c$).

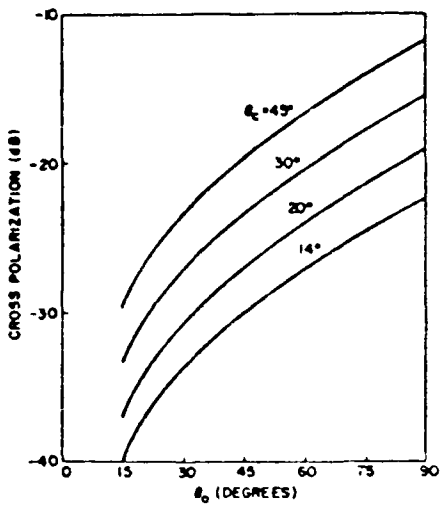

Figure 22. Maximum cross polarization of linearly polarized excitation.

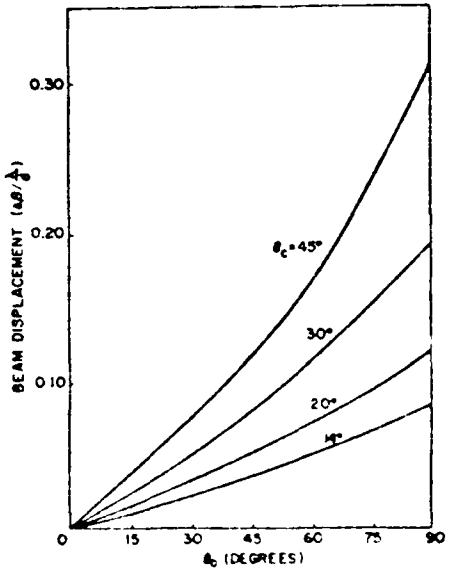

Figure 23. Beam displacement of circularly polarized excitation (no circular cross polarization.

Figures 21-23 after Chu and Turrin,[21] copyright 1973 by IEEE.

circularly polarized beams are squinted on opposite sides of boresight in the offset plane of the reflector. This effect can be reduced by increasing the focal length of the reflector or it can be compensated for in the data reduction process.

2. CASSEGRAIN

A Cassegrain antenna is a double reflector antenna consisting of a paraboloidal main reflector and a hyperboloidal sub-reflector. One of the major advantages of a Cassegrain antenna is that its folded optics system produces a more compact mechanical structure than does a paraboloid antenna for equivalent focal lengths. The other major advantage of the Casegrain antenna is that the feed and the microwave plumbing are conveniently located behind the main reflector, presenting no blockage and providing easier access to these components than in a front-feed paraboloidal antenna.

Hannan[22] and Wong[23] have shown that the performance of a Cassegrain antenna is the same as that of an equivalent paraboloid antenna; therefore Figures 20 through 23 can also be used for a Cassegrain antenna by inserting the equivalent focal length for f. Since the focal length of the equivalent paraboloid antenna is usually much larger than that of the focal length of the main reflector, the cross-polarization properties of the Cassegrain antenna will be superior. Again, an offset geometry eliminates feed and sub-reflector blockage and, thus produces superior electrical performance at the expense of a more complex and hence costly, mechanical sturcture.

[22] Hannan, P. W., 1961: Microwave Antennas Derived from the Cassegrain Telescope, IRE Trans. Antennas Propag., AP-9, 140-153.

[23] Wong, W. C., 1973: On The Equivalent Parabola Technique To Predict The Performance Characteristics of a Cassegrainian System With an Offset Feed, IEEE Trans. Antennas Propag., AP-21, 168-172.

B. FEEDS

The type of feed used with a reflector antenna can have a significant affect on the overall cross-polarized performance of the antenna. Typical feeds for reflector antennas include dipoles, pyramidal horns, and multi-mode horns. The behavior of each of these with a paraboloidal reflector is described below. A Cassegrain antenna can be analyzed in terms of an equivalent paraboloid[22,23] and so is not explicitly treated here.

1. DIPOLE FEEDS

Dipole feeds are typically used at VHF frequencies and below, although they have been used for some applications at microwave frequencies. Dipoles are generally unsatisfactory from a practical point of view since they have unequal E-plane and H-plane beamwidths and have high backlobe radiation. Combining several dipoles into an array can reduce the backlobe radiation and provide beamwidth control to obtain tapered illumination of the reflector. The resulting feed, however, is relatively narrowband. Dual, linearly polarized operation can be obtained by separately feeding two crossed dipoles. Dipole feeds are popular from a theoretical point of view since they are relatively easy to analyze. Dipole feeds are not recommended for the intended application due to the practical difficulties just mentioned.

2. PYRAMIDAL HORNS

The pyramidal horn is the most commonly used feed for reflector antennas at microwave frequencies since it allows independent control of the E-plane and H-plane illuminations of the reflector. Dual linear polarization can be obtained by exciting a pyramidal horn with a commercially available dual mode transducer. Dual circular polarization is discussed under the RF plumbing section. Figure 20 shows that a pyramidal horn will produce a 2 to 4 dB improvement in peak cross polarization over a dipole feed.

3. MULTI-MODE HORNS

Figure 10 shows that the cross-polarized radiation from a paraboloid can be reduced to very small levels by using a corrugated horn

enough focal length. Because such an approach may produce an antenna that is too large, alternate approaches have been considered by a number of investigators. If a proper combination of waveguide modes could be generated in a feed, a cross-polarization-free antenna could (theoretically) be obtained; a number[24,25] of different designs have been proposed and implemented to accomplish this.

In the so-called Potter horn,[24] the sidelobes and cross-polarized energy radiated by the TE_{11} mode of a circular aperture are partially cancelled by adding in opposite phase a small portion of TM_{11} mode which has nearly identical sidelobes and cross-polarized patterns. Potter generated this higher order waveguide mode by using a discontinuity in the slope of the inside wall of a conical horn.

The Potter feed works reasonably well for center fed reflectors. For offset reflectors, however, a third mode must be added as shown by Rudge[25]. Rudge presented experimental data showing that his tri-mode feed can give as much as 20 dB cross-polarization suppression over that achievable with a Potter type feed.

C. RF PLUMBING

Two RF channels are required for the system: one for carrying transmitter power to the antenna and this same channel and one other for carrying received signals from the antenna to the two receivers. Both of these channels must be phase and amplitude matched. If both the receivers and the transmitter are located below the pedestal, then two dual channel rotary joints are needed, one for the azimuth axis and one for the elevation axis. Rotary joints have notoriously bad phase tracking charac-

[24] Potter, P. D., 1963: A New Horn Antenna with Suppressed Sidelobes and Equal Beamwidth, Microwave Journal, VI, (No. 6), 71-78.

[25] Rudge, A. W. and Adatia, N. A., 1978: Offset-Parabolic-Reflector Antennas: Review, Proc. IEEE, 66, 1592-1618.

teristics. This problem combined with long waveguide runs from the feed to the transmitter and receivers indicates that the receivers should be mounted on the antenna. Only by mounting the receivers on the antenna, and preferably at the feed, can adequate phase and amplitude accuracy be obtained, as is required for good cross-polarization performance.

D. DUAL-POLARIZATION GENERATION

A dual-polarized feed can be implemented in a number of ways including a dual mode transducer or a turnstile junction input to a waveguide horn. The dual mode transducer approach is recommended because it handles high power, has good phase and amplitude matching, and provides good isolation between ports. In addition, these units are available off-the-shelf in most waveguide bands. This approach is also more broadband than the turnstile junction.

The feed itself can be either dual linearly polarized or dual circularly polarized. Dual linear polarization is produced naturally by the dual mode transducer. An exciting network for the feed is shown in Figure 24 and would allow any sense elliptical, circular or linear polarization to be radiated by the feed. The sense of polarization is changed by changing the phase shifter settings. Each receiver receives one of two orthogonally polarized signals.

E. FREQUENCY BAND CONSIDERATIONS

Both K_a-band and X-band operations were initially considered. The free space wavelength is 8.6 mm at 35 GHz and 10 cm at 3 GHz. A 1° beamwidth antenna would be about 2 m in diameter at 3 GHz and 0.6 m in diameter at 35 GHz. Reflectors with accurate surfaces can be made at either frequency. Dual-mode transducers are available on both bands and feed can be made to both bands. Waveguide losses are 0.096 dB m^{-1} at 3 GHz and 0.57 dB m^{-1} at 35 GHz. Thus, the 35 GHz transmitter and receivers need to be located at the antenna if excessive waveguide losses are to be avoided.

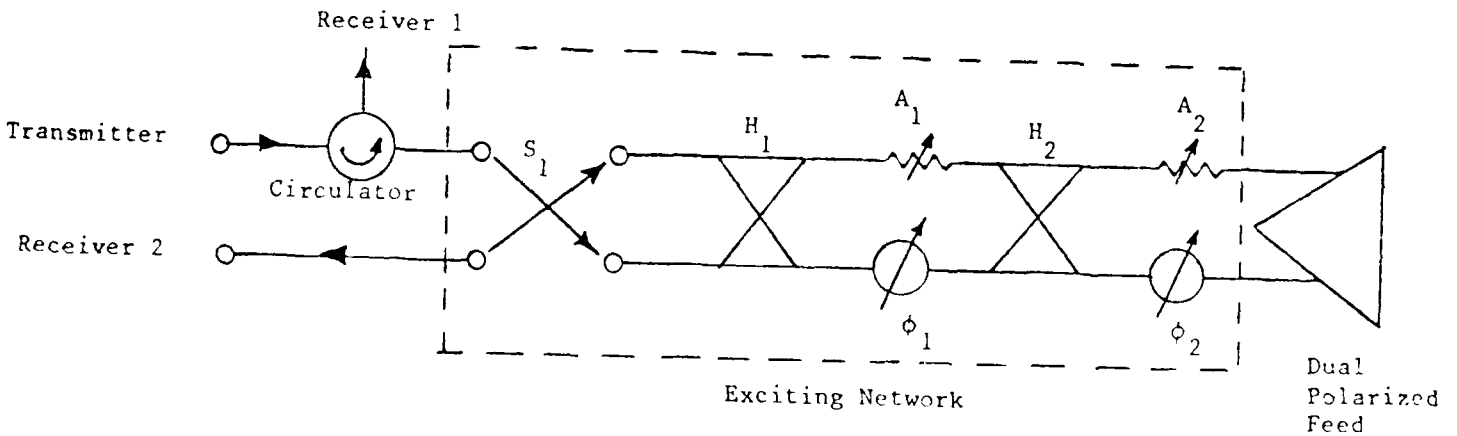

H_1, H_2 = 3dB hybrids

A_1, A_2 = trimmer attenuators

ϕ_1, ϕ_2 = phase shifters

S_1 = double pole, transfer switch

Figure 24. Exciting network for dual polarized feed.

There appear to be no practical or theoretical limitations in building the antenna for either band.

F. RECOMMENDATIONS FOR OPTIMUM SYSTEM

The preceding evaluation supports the following recommendations for the optimum antenna system. A [illegible] reflector in conjunction with a highly tapered [illegible] is required to produce low cross-polarized [illegible]. The feed should be a partially offset feed geometry to reduce the effects of aperture blockage. A multimode feed should be used for improved cross-polarized performance. The antenna can be built at either K_a- or S-band.

The above design approach has been demonstrated to produce peak cross-polarized lobes that are at least 35 dB bc. the peak response of the co-polarized pattern and to have a null on boresight. For comparison purposes, the reported cross-polarized level of the antenna used by the National Research Council of Canada at Ottawa is 28 dB. Georgia Tech has built a number of antennas having 33 dB to 35 dB cross-polarized peaks, but these antennas were not designed for optimum cross-polarized performance. The integrated cancellation ratio will be substantially better than the peak cross-polarized lobe level since this ratio averages the cross-polarized to co-polarized response of the antenna across the entire main lobe.

G. USE OF EXISTING ANTENNA

A portion of the antenna analysis dealt specifically with the X-band antenna that had been acquired by AFGL. The antenna is a center-fed, 7.3-m diameter paraboloid having a 7.9-m focal length. Antenna patterns were calculated for this antenna using a computer code originally developed at Georgia Tech. Calculated values agreed well with measured data provided by AFGL for the co-polarized pattern. No cross-polarized data, however, were available. The predicted level of the cross-polarized energy for this antenna was -24 dB. Thus, this antenna is about 10 dB worse

in cross-polarized performance than the optimum antenna recommended in Subsection F.

The S-band antenna should be modified in one of the following three ways to permit simultaneous dual polarized operation:

1. Center feed paraboloid with receivers at the focal point.
2. Center feed paraboloid with receivers located behind the reflector.
3. Cassegrain reflector with receivers behind the reflector.

These three options need to be examined in terms of blockage, polarization accuracy, mechanical compatibility, and cost to determine the most desired approach. The advantages and disadvantages of a dual linear versus a dual circularly polarized feed for the S-band antenna should be delineated. The effects of a metal space frame radome on the polarization performance of the radar should also be analyzed. These effects might establish a limit on achievable cross-polarization performance.

SECTION VI
DATA PROCESSING AND RADAR CONTROL

A. CONCEPTS

The detailed data processing requirements will be determined by the measurement scenario, i.e., the type of scattering medium under observation and the scanning mode of the radar. In general, the data processing will include the computation of average parameters of the received signals such as average power, mean Doppler velocities, cross-covariance of the two received signals, and parameters derived from these and the computation of the corresponding spectral functions, namely, the two power spectra, the cross-spectrum, and other functions derived from these. The average parameters can be computed in real-time for display and recorded for later study. The computation of spectral functions in real-time will require larger computational capacity, and can probably be done more effectively off-line if such analysis is required in more than a few range gates.

The basic measurement capabilities of a coherent circularly-polarized dual-channel radar are summarized in Table 8. Here W_1 and W_2 are the received powers in the parallel polarization (transmission channel) and cross-polarization (opposite channel), respectively, and W is the cross-covariance, following the notation of McCormick and Hendry[1]. S_1 and S_2 are the corresponding power spectra and S_{12} is the cross-spectrum of the two received signals. The table also indicates the subsidiary measurement capabilities of a non-coherent dual-channel radar and a coherent single-channel radar. (Because the larger circularly polarized signal is received in the cross-polarized channel, it is W_2 and S_2 that are equivalent to the average power and power spectrum obtained from a single-channel linearly-polarized coherent radar.) From these basic parameters and functions one can form the circular depolarization ratio W_1/W_2, the cross-correlation $W/(W_1W_2)^{1/2}$, the quantity W/W_2 which is useful in the study of

propagation effects, and the spectral counterparts of all these quantities.

TABLE 8. MEASUREMENT CAPABILITIES OF A COHERENT DUAL-CHANNEL RADAR

	Non-coherent dual-channel	
	W_1	$S_1(f)$
Coherent Single-channel	W_2	$S_2(f)$
	W	$S_{12}(f)$

The maximum utility of the coherent dual-channel radar can be realized in conditions under which the Doppler velocity contains a significant component due to fall speed, so that variations in Doppler velocity can be related to variations in hydrometeor size. These conditions require (1) that some fraction of the detectable hydrometeors be precipitation-sized, and (2) that the observations be made at a relatively high elevation angle, i.e., in the primary coverage region discussed in Section III. The spectral functions will be most useful under these conditions. At low elevation angles, the spectrum width will be determined mainly by wind shear and turbulence, and the backscattered signals due to hydrometeors of any given size will appear distributed across the spectrum. One would expect under these conditions that the spectral power ratio S_1/S_2 and the spectral cross-correlation $S_{12}/(S_1S_2)^{1/2}$ will be uniform functions of Doppler frequency and hence contain no information beyond that contained in the circular depolarization ratio W_1/W_2 and the cross-correlation $W/(W_1W_2)^{1/2}$.

A given set of experimental objectives will determine a scanning mode, e.g., in azimuth at fixed elevation, or in elevation at fixed azimuth. We recommend that the scanning mode be under computer control and that the control unit incorporate several pre-programmed scan sequences with corresponding data-processing functions. For example, the computation of mean Doppler velocity for both channels might be desirable in the case of observations at high elevation angles whereas these would be redundant at low elevation angles. The operater would then select an operating mode, specify certain parameters, such as the angular limits on a sector scan, and select certain quantities to be computed and displayed.

E. IMPLEMENTATION

The block diagram of Figure 25 presents a dual processor approach to monitoring the radar and data recording. The two color displays/terminals use identical hardware. The radar control unit operates in a real-time priority interrupt mode; it controls radar parameters, specifies scanning patterns, etc. The data processing unit operates in non-real-time; it performs signal processing operations for data verification or analysis.

The recording and sampling of the data are controlled by the radar control unit; the actual parameter selections are input by the user from the terminal. The low data rate quantities such as antenna position, range gate positions, sampling configuration, etc., are recorded on a digital tape. The actual return signal is recorded on a wideband tape unit. The specification of this wideband unit as to analog or digital remains to be determined; both are compatible.

If the microprocessors are chosen fast enough, the radar control unit could conceivably have enough capability to process and display data in simple formats (i.e., amplitude versus range) and statistical summaries (i.e., mean and variance estimates, etc.).

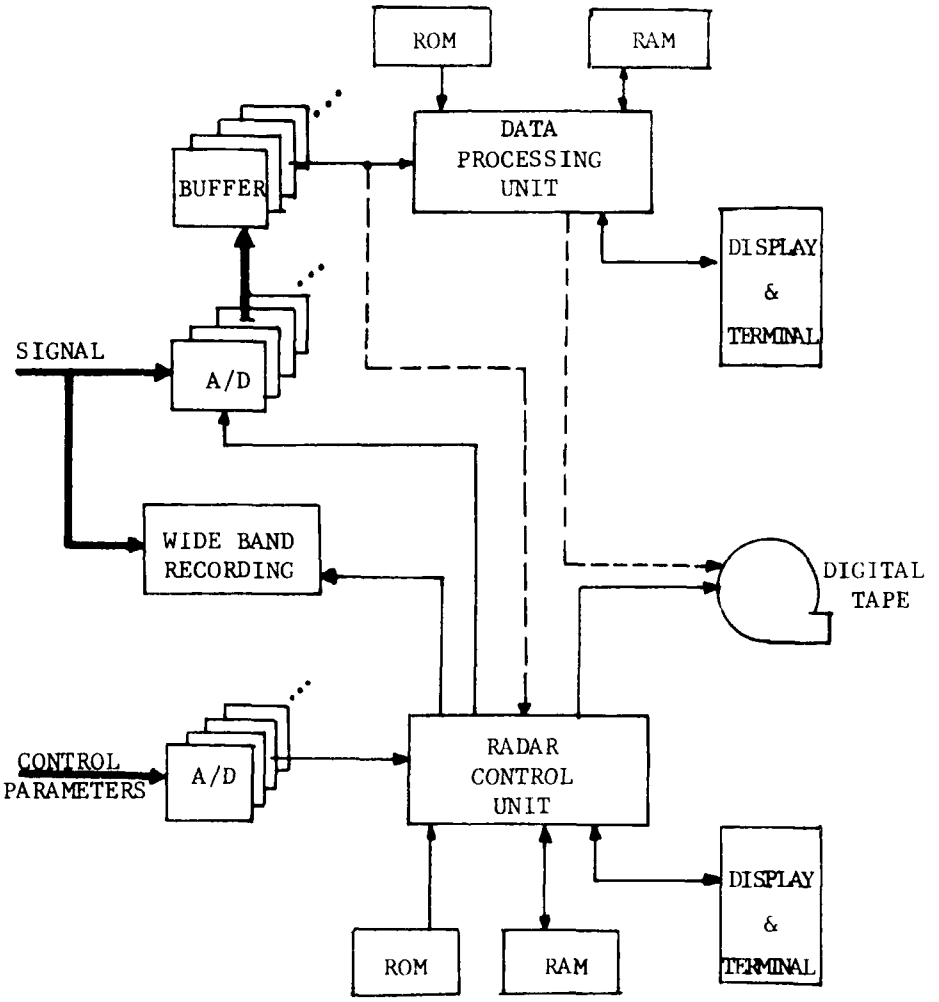

Figure 25 Block diagram of radar control and data processing system.

The data processor unit selects, via user control, an algorithm or set of algorithms to process the data. Depending on the processor speed, with cost proportional to an increase in speed, some or all of the available algorithms can be run in near-real-time. Outputs from the data processor unit can be displayed in color. For example:

1. Color coded amplitude or intensity versus range on an azimuth scan (PPI).
2. Amplitude versus range at fixed azimuth/elevation position, both polarizations.
3. Spectral data in scanning or fixed modes, single or both polarizations.
4. Correlation quantities.

There is an implementation cost savings in using the dual unit approach. A set of real-time software and non-real-time software is needed no matter what approach is used, but, in the single processor concept, both must be made to operate together with appropriate links and priorities. With the dual processor approach, the linking software need not be developed, and more efficiency can be built into each unit. Two color displays allow more complete knowledge of radar performance and data verification. With interchangeable microprocessors, the malfunction of one unit still permits radar operation and data collection.

SECTION VII
CONCLUSIONS AND RECOMMENDATIONS

A. CONCLUSIONS

Two radar systems of similar configuration, operating at widely different transmitting frequencies, are postulated for measurement of hydrometeor polarization characteristics. An S-band radar is optimum for measurements of backscatter from hydrometeors in a precipitation medium. A K_a-band radar is optimum for measurements of backscatter from clouds through a clear medium. The primary criterion for operating frequency was the radar preprocessing detection capability, expressed in terms of signal-to-noise ratio, at the maximum range of measurements. Additional criteria included propagation effects and the operational scenario, e.g., long-range surveillance or short-range measurement of Doppler frequency-related parameters.

The lower frequency regime has the advantages of long-range detection, low signal attenuation even in heavy rain, and low depolarization due to differential attenuation and differential phase shift along the propagation path. Thus at S-band, the parameters derived from the received signals in most cases are valid representations of the scattering medium. The operational capabilities of such a radar include measurement of Doppler wind speed (as with a single-channel coherent radar), derivation of raindrop size distributions, separation of Doppler components due to fall speed and to air velocity in some cases, and detection of hail in rain. Discrimination of snow and rain is possible on the basis of differing fall speeds and reflectivity, although the capability for measuring polarization parameters in snow would be limited. If transmitted power is high enough, e.g., several hundred kilowatts, detection of clouds will be possible at short ranges.

The higher frequency regime (K_a-band) is necessary to obtain adequate signal-to-noise ratios for backscatter from clouds. Use

of K_a-band will permit measurement of Doppler velocity parameters in clouds and discrimination between ice and liquid cloud particles. Estimates of target size and number density will be based on reflectivity derived from the "main" channel signal. If the ice crystals are strongly oriented by aerodynamic or electrical forces, then additional information can be derived from the scattering and propagation parameters. The interpretation of such measurements will depend strongly on the measurement scenario and the physical processes affecting the propagation and scattering media. At very short ranges, a K_a-band radar is capable of measuring scattering parameters in rain. This capability overlaps that of an S-band radar, but is complicated at K_a-band due to Mie scattering effects and to propagation effects which increase rapidly with range.

The coherent dual-channel radar offers several advantages over the joint use of a coherent single-channel radar and a non-coherent dual-channel radar. The measurement of dynamical and physical parameters by a single radar allows considerable simplification of system design and operation. In addition to the Doppler spectrum and average signal parameters, information is available from the coherent dual-channel radar through the spectral power ratio, S_1/S_2, and the cross-spectrum, S_{12}. These spectral functions contain information on the distribution of shapes, sizes, and orientation parameters of the hydrometeors. If hydrometeor fall speed contributes significantly to the Doppler frequency spread of the received signals, as could occur in rain, then measured shape parameters can be related to raindrop size. In clouds and in radar observations at low elevation angles, the Doppler frequency spread should be dominated by turbulence or wind shear, and the backscatter characteristics associated with any particular size or type of hydrometeor should be distributed across the frequency domain of the signals. In these situations, the spectral power ratio and the cross-spectrum can be expected to yield no information beyond that derivable from the depolarization ratio and the cross-covariance. Any deviation

in these functions from the expected frequency-independence, however, should yield some information on microphysical parameters.

A radar operating at either S-band or K_a-band should have a pulse width of 0.5 to 2.0 us, a beamwidth of 0.5 to 2.0 degrees, a peak transmitted power of at least 100 kW, a pulse repetition frequency variable between 300 Hz and 10 kHz, and full scanning capability in azimuth and elevation angles. Operation in a single freqency band is sufficient for observation of the polarization characteristics of precipitation or clouds at S-band or K_a-band, respectively. Current technological capabilities in radar components are sufficient to achieve these specifications. In particular, antenna designs can be developed which should give dual-polarization performance (purity across beam, isolation between channels) better than that achieved by meteorological research radars at present.

B. RECOMMENDATIONS

We recommend that serious consideration be given to the development of radar systems at both S-band and K_a-band for measurement of hydrometeor microphysical parameters in precipitation and clouds. Our investigation has shown that such development is technologically feasible and will yield significant advances in meteorological measurement capability. As the development of new radar systems proceeds, experimental programs should be conducted using existing radars having some of the capabilities discussed in this report. Such programs will permit the development of analytical techniques, the determination of the utility of various derived parameters and functions for research or operational purposes, and the evaluation of particular radar performance parameters.

In addition to the use of existing radars for experimental programs, the possibility of modifying existing radars to achieve the coherent dual-channel measurement capability should be given detailed study. In particular, our preliminary evaluation of the

S-band Doppler radar being installed by Air Force Geophysics Laboratory indicates that this radar can be modified to yield satisfactory performance as a dual-channel system. This approach to the radar system development offers the advantages of using components of the existing radar and using the AFGL data processing system for much of the real-time processing and display. The further study of this development option must address (1) the expected performance limits associated with particular technical approaches, (2) logistical considerations, (3) calibration and error-compensation procedures, and (4) specific requirements for real-time displays and off-line data processing.

REFERENCES

1. McCormick, G. C., and A. Hendry, 1975: Principles for the Radar Determination of the Polarization Properties of Precipitation. Radio Sci., 10, 421-434.

2. Metcalf, J. I., and J. D. Echard, 1978: Coherent Polarization-Diversity Radar Techniques in Meteorology. J. Atmos. Sci., 35, 2010-2019.

3. Metcalf, J. I., S. P. Brookshire, and T. P. Morton, 1978: Polarization-Diversity Radar and Lidar Technology in Meteorological Research: A Review of Theory and Measurements. AFGL-TR-78-0030, Air Force Geophysics Laboratory.

4. Humphries, R. G., 1974: Depolarization Effects at 3 GHz Due to Rain. Sci. Rept., MW-82, Stormy Weather Group, McGill University.

5. Warner, C. W., and R. R. Rogers, 1977: Polarization-Diversity Radar: Two Theoretical Studies. Sci. Rept. MW-96, Stormy Weather Group, McGill University.

6. Oguchi T., and Y. Hosoya, 1974: Scattering Properties of Oblate Raindrops and Cross Polarization of Radio Waves Due to Rain (Part II): Calculations at Microwave and Millimeter Wave Regions. J. Radio Res. Labs. (Japan), 21, 191-259.

7. Metcalf, J. I., 1980: Propagation Effects on a Coherent Polarization-Diversity Radar. 19th Conf. Radar Meteor., Amer. Meteor. Soc.

8. Battan, L. J., 1973: Radar Observation of the Atmosphere. University of Chicago Press.

9. Marshall, J. S., and W. M. Palmer, 1948: The Distribution of Raindrops with Size. J. Meteor., 5, 165-166.

10. Wexler, R., and D. Atlas, 1963: Radar Reflectivity and Attenuation of Rain. J. Appl. Meteor., 2, 276-280.

11. Douglas, R. H., 1964: Hail Size Distribution. Proc. 11th Wea. Radar Conf., Amer. Meteor. Soc., 146-149.

12. Atlas, D., 1954: The Estimation of Cloud Parameters by Radar. J. Meteor., 11, 309-317.

13. Van Vleck, J. H., 1947: Absorption of Microwaves by Oxygen and The Absorption of Microwaves by Uncondensed Water Vapor. Phys. Rev., 71, 425-433.

14. Burrows, C. R., and S. S. Atwood, 1949: Radio Wave Propagation. Consolidated Summary Technical Report of the Committee on Propagation, NDRC, Academic Press, New York.

15. Derr, V.E., 1978: A Basic Comparison of Lidar and Radar for Remote Sensing of Clouds. Technical Report ERL 397-WPL 52, Nat'l. Oceanic and Atmospheric Admin.

16. McCormick, G. C., and Hendry, A., 1979: Techniques for the Determination of the Polarization Properties of Precipitation. Radio Sci., 14, 1027-1040.

17. Krehbiel, P. R., and Brook, M., 1979: A Broad-Band Noise Technique for Fast-Scanning Radar Observations of Clouds and Clutter Targets. IEEE Trans. Geosci. Electr., GE-17, 196-204.

18. McCormick, G. C., and Hendry, A., 1979: Radar Measurement of Precipitation-Related Depolarization in Thunderstorms. IEEE Trans. Geosci. Electr., GE-17, 142-150.

19. Jones, E. M. T., 1954: Paraboloid Reflector and Hyperboloid Lens Antennas, IRE Trans. Antennas Propag., AP-2, 119-127.

20. Bodnar, D. G., 1980: Cross-Polarized Characteristics of Monopulse Difference Patterns, IEEE/AP-S Int'l. Symp., Quebec, Canada, June 2-6.

21. Chu, T. S. and Turrin, R. H., 1973: Depolarization Properties of Offset Reflector Antennas, IEEE Trans. Antennas Propag., AP-21, 339-345.

22. Hannan, P. W., 1961: Microwave Antennas Derived from the Cassegrain Telescope, IRE Trans. Antennas Propag., AP-9, 140-153.

23. Wong, W. C., 1973: On The Equivalent Parabola Technique To Predict The Performance Characteristics of a Cassegrainian System With an Offset Feed, IEEE Trans. Antennas Propag., AP-21, 168-172.

24. Potter, P. D., 1963: A New Horn Antenna with Suppressed Sidelobes and Equal Beamwidth, Microwave Journal, VI, (No. 6), 71-78.

25. Rudge, A. W. and Adatia, N. A., 1978: Offset-Parabolic-Reflector Antennas: Review, Proc. IEEE, 66, 1592-1618.

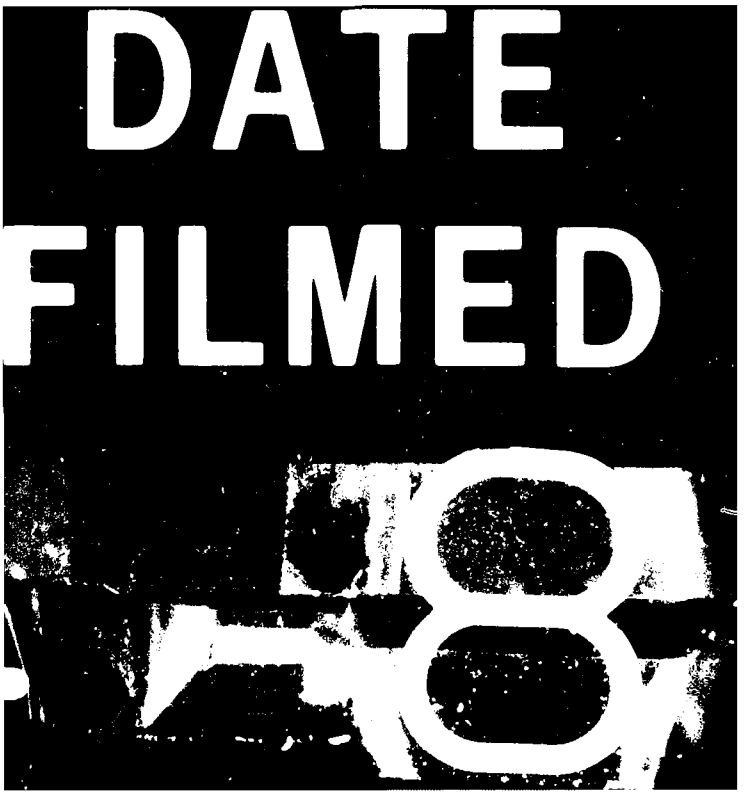
DATE
FILMED